

**STUDY OF THE ELECTROPLATING COATING OF
Zn-Ni ALLOY ON LOCALLY MANUFACTURED
MILD STEEL PLATE**



BY

**MD. MOKARRAM HOSSAIN
ROLL NO. 9005**

**Thesis submitted to the Department of Chemistry,
Bangladesh University of Engineering & Technology
(BUET) for the Partial Fulfillment of**

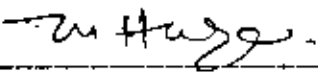

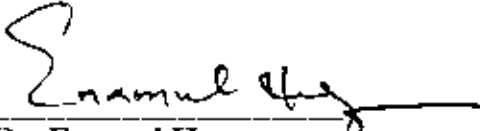
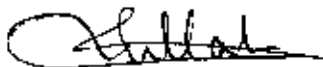
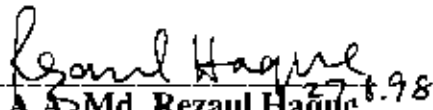
**M. Phil. Degree
in
Chemistry**

August 1998



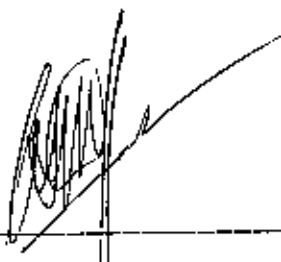
THESIS APPROVAL SHEET

Thesis entitled "Study of the Electroplating Coating of Zn-Ni Alloy on Locally Manufactured Mild Steel Plate", submitted by Md. Mokarram Hossain is approved for the degree of Master of Philosophy.

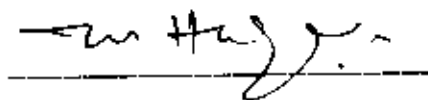
1. 
Dr. Md. Monimul Huque
Professor
Department of Chemistry
BUET, Dhaka. Supervisor & Chairman
Examination Committee
2. 
Dr. A.S.M.A. Haseeb
Associate Professor
Department of Materials and Metallurgical
Engineering, BUET, Dhaka. Co-supervisor
3. 
Dr. Enamul Haq 27.8.98
Professor & Head
Department of Chemistry
BUET, Dhaka. Member
4. 
Dr. Md. Rafique Ullah 27.8.98
Associate Professor
Department of Chemistry
BUET, Dhaka. Member
5. 
Dr. A.S.Md. Rezaul Haque 27.8.98
Professor & Head
Department of Materials and Metallurgical
Engineering, BUET, Dhaka. External Member

DECLARATION CERTIFICATE

Certified that the work incorporated in this thesis "**Study of the Electroplating Coating of Zn-Ni Alloy on Locally Manufactured Mild Steel Plate**" submitted by Md. Mokarram Hossain has been carried out by the candidate under our supervision. The work embodied in this thesis is original and we declare that it has not been submitted in part or in full for the award of any degree or diploma.



Co-supervisor



Supervisor

ACKNOWLEDGMENT

I would like to express my gratitude and indebtedness to my thesis supervisor Prof. Dr. Md. Monimul Huque, Department of Chemistry, BUET for his inspiring guidance, constant encouragement in successful completion of the research work.

I am specially indebted and much grateful to my thesis co-supervisor Dr. A.S.M.A. Haseeb, Associate Professor, Department of Materials and Metallurgical Engineering, BUET for his kind assistance through proper suggestions in carrying out the research work as well as in writing the thesis.

I acknowledge the contribution of Head, Chemistry Department, Head Materials and Metallurgical Engineering Department of BUET and Principal, Madrasa-e-Alia, Dhaka.

I am grateful to Prof. Dr. M. Feroze Ahmed, Department of Civil Engineering, BUET for allowing me to carry out atomic absorption spectroscopic analysis.

I express thanks to Mr. Md. Moniruzzaman, Asstt. Professor, Department of Materials and Metallurgical Engineering, BUET, Dhaka for his valuable co-operation. I am grateful to Mr. Md. Yousuf Khan, Instrument Engineer (Elect), for his help in using the X-ray Diffractometer.

Thanks to Mr. Nazrul Islam Mandal, Technician, Chemistry Department, Mr. Ashiqur Rahman, Senior Laboratory Instructor and Mr. Binoy Bhushan Saha, Senior laboratory Instructor, Department of Materials and Metallurgical Engineering, BUET and all the staffs of the Chemistry Department for their help in various stages of the study.

Finally, I must thank my wife, Shahana Yasmin and my parents for their encouragement during research work for this thesis.


(Md. Mokarram Hossain)

ABSTRACT

Zinc-nickel alloy coatings have drawn considerable interest in recent years because of their improved corrosion resistance as compared with zinc coating. The present work attempts to investigate the electrodeposition of zinc-nickel alloy coatings and study their corrosion behaviour. Deposition of pure zinc coating was also done and its corrosion behaviour studied for comparison purposes.

The deposition of zinc-nickel alloy coating on mild steel was carried out galvanostatically in sulphate based baths in the current density range of 40-80 mA/cm². Deposition was carried out in the pH range of 2-4 and at temperatures 25°C and 45°C. The Zn-Ni alloy coating was chemically analysed for nickel content mainly by atomic absorption spectroscopy and also by wet chemical method. The thickness of the coating was determined under optical microscope. X-ray diffraction studies were carried out on the coatings in the as-deposited and annealed conditions to find out the phase structure. Corrosion behaviour of both pure zinc and Zn-6%Ni alloy coatings on mild steel were investigated using hot water and salt water immersion tests and electrochemical corrosion tests. Electrochemical corrosion test were done in various media containing different amount of NaCl, Na₂S and FeCl₃.

Bath pH was found to have a large effect on the quality of the zinc-nickel alloy coatings. Uniform and adherent coatings were obtained in the pH range of 2-4. The nickel content of the deposit was observed to be influenced by bath composition and temperature. Nickel content of the deposit was found to increase linearly with the percentage of nickel in the bath. However, nickel, in spite of being more noble, was found to deposit less readily than zinc. Thus co-deposition of zinc and nickel is seen to be of the anomalous type. Increasing bath temperature has the effect of increasing nickel content of the deposit. Nickel content of the desposits from baths containing lower nickel percentage was found to be independent of deposition current density. However, for the bath containing a high percentage of nickel, slight increase in the nickel content of the deposit was observed with increasing current density. X-ray diffraction shows the as deposited coatings are in a stressed state.

Salt water immersion tests showed that it took 120 days to form red rust on Zn-6%Ni alloy coating whereas it took only 55 days for pure zinc. It was further seen that after an exposure period of 12 days, corrosion rate of zinc-nickel alloy coating was found to be one-third that of pure zinc coating.

Anodic polarization behaviour revealed that the corrosion rate of Zn-6%Ni alloy coating was lower than that of zinc coating in all the media investigated. Annealed Zn-6%Ni alloy coating was found to be more corrosion resistant than the as-deposited coating.

CONTENTS

ACKNOWLEDGEMENT

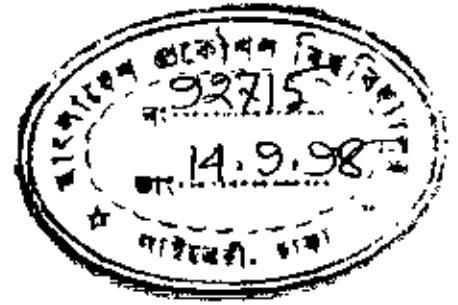
ABSTRACT

CHAPTER 1: INTRODUCTION	1
CHAPTER-2: LITERATURE REVIEW	3
2.1 Fundamentals of electrodeposition	3
2.2 Principles of alloy electrodeposition	7
2.2.1 Introduction	7
2.2.2 Static potential and electrodeposition of alloys	8
2.2.3 Criteria for electrodeposition of alloy	15
2.3 Electrodeposition of zinc-alloys	17
2.3.1 Effect of plating variables on the composition of zinc-alloy deposit	22
2.3.1.1 Effect of bath composition	22
2.3.1.2 Effect of current density	23
2.3.1.3 Effect of temperature	27
2.3.1.4 Effect of pH	28
2.4 Corrosion testing	28
2.4.1 Introduction	28
2.4.2 Purposes of corrosion testing	29
2.4.3 Surface preparation for corrosion testing	30
2.4.4 Measuring and weighing	33
2.4.5 Exposure techniques	33
2.4.6 Standard expression for corrosion rate	34
2.4.7 Classification of corrosion testing	34
2.4.8 Immersion test	35

2.4.8.1	Salt (3% NaCl) solution immersion test	35
2.4.8.2	Hot water immersion test	36
2.4.9	Electrochemical test	37
2.4.9.1	Polarization Techniques for Estimating Corrosion current	37
2.4.9.2	Polarization resistance	42
2.4.9.3	Small amplitude polarization techniques	45
2.4.9.4	General polarization techniques	45
CHAPTER-3:	EXPERIMENTAL	49
3.1	Electrodeposition	49
3.1.1	Preparation of the substrate for electrodeposition	49
3.1.2	Electrodeposition set-up	51
3.1.3	Electroplating operation	53
3.2	Chemical analysis of coatings	54
3.2.1	Chemical analysis by atomic absorption spectroscopy	54
3.2.2	Analysis by conventional wet chemical method	55
3.3	Determination of coating thickness	56
3.4	X-ray diffraction studies	56
3.5	Corrosion test	57
3.5.1	Salt water immersion test	57
3.5.2	Hot water immersion test	59
3.5.3	Electrochemical corrosion test	59

CHAPTER-4: RESULTS AND DISCUSSION	61
4.1 Electrodeposition of zinc-nickel alloy	61
4.1.1 Effect of deposition current density	61
4.1.2 Effect of bath composition	63
4.1.3 Effect of bath temperature	65
4.1.4 Effect of pH	66
4.1.5 Phase structure of coatings	67
4.2 Corrosion behavior of zinc and zinc-nickel alloy coatings	70
4.2.1 Corrosion in hot water	71
4.2.2 Salt water corrosion	72
4.2.3 Electrochemical corrosion	75
CHAPTER-5: SUMMARY AND CONCLUSION	90
REFERENCES	94

CHAPTER-ONE



Introduction

The resistance of mild steel to corrosion in humid atmosphere is very low. Corrosion of mild steel becomes severe in chloride containing environments specially in coastal areas. In order to protect mild steel from such corrosion, hot dipped galvanized zinc coatings have traditionally been used. However, during the last decade, there has been an increased demand for electrodeposited zinc coatings particularly by automakers¹. Electrodeposition of zinc coating offers a number of advantages. It is amenable to accurate process control which leads to a uniform product quality and higher productivity. Electrogalvanized coatings also act as a good base for subsequent painting as is required in automobile and other applications.

Recently electrodeposited zinc-nickel alloy coatings have attracted a great deal of attention because they can offer a higher degree of corrosion resistance and better mechanical properties than pure zinc coatings². Substantial improvements are obtained even with small percentages of the more expensive nickel and potential economic advantages in using zinc-nickel alloy instead of zinc coatings have been recognized².

In the present work, attempt has been made to study electrodeposition of zinc-nickel alloy coatings of locally produced mild steel substrate in sulphate based baths. Effect of various

parameters like bath composition, deposition current density, bath temperature, pH etc. on the characteristics of the coatings have been investigated. In the second part of the work, a comprehensive investigation on the corrosion behaviour of zinc-nickel alloy has been made using immersion and electrochemical methods. Corrosion behaviour of zinc-nickel alloy coating is also compared with that of electrodeposited pure zinc coatings.

CHAPTER: TWO

2. Literature Review

2.1 Fundamentals of Electrodeposition

In an electrodeposition cell, a reaction of the type



can take place at the cathode. The metal electrode consists of metal ions in a crystal structure. The transfer of a metal ion from the electrolyte structure to the metal structure will be accompanied by a free energy change ΔG . Thermodynamics tells that in a system with only PV work, the free energy changes for the transport of n moles of matter i from phase 1 to phase 2 according to

$$dG = VdP - SdT + \mu^2_i dn - \mu^1_i dn \quad \dots\dots\dots(2.2)$$

where μ^1_i and μ^2_i are the chemical potentials in phase 1 and 2 respectively, in an electrochemical system, not only PV-work, but also electrical work — the work accompanying the transport of electrical charge over a potential difference — must be taken into account. Equation 2.2 then transforms into

$$dG = VdP - SdT + (\mu^2_i - \mu^1_i)dn + (\phi^2_i - \phi^1_i)zFdn \quad \dots\dots(2-3)$$

where $zF(\phi^2_i - \phi^1_i)$ is the electrical work involved in the transport of the electrical charge of 1 mole of ions from phase 1 to phase 2, ϕ is the electrical potential and F is Faraday's constant. The equilibrium

criterion, with P and T constant, is that the free energy is minimum, thus $dG=0$ and consequently $\mu^1_i = \mu^2_i$. So the condition for equilibrium is now [from (2-3)]

$$\mu^1_i + zF\phi^1_i = \mu^2_i + zF\phi^2_i$$

$$\mu_i^{E1.1} = \mu_i^{E1.2}$$

For the electrochemical reaction, [Eq. 2.1], taking place at the electrode:

$\Delta\phi_e = \phi_M - \phi_s$ [where $\Delta\phi_e$ = Potential difference between the metal at the electrode and its ions in solution] and

$$\Delta G^{E1} = \Delta G^0 - RT \ln a_{M^{z+}} + zF\Delta\phi_e \dots \dots \dots (2.4)$$

where ΔG^0 = Standard free energy of reaction (2.1)

$a_{M^{z+}}$ = Activity of M^{z+}

Under standard conditions ($a_{M^{z+}} = 1$) at equilibrium.

$$\Delta G^{E1} = 0 \text{ and } \Delta\phi_e = \Delta\phi_e^0$$

Hence (2.4) transforms to

$$0 = \Delta G^0 - 0 + zF\Delta\phi_e^0$$

$$\Rightarrow \Delta G^0 = -zF\Delta\phi_e^0 \dots \dots \dots (2.5)$$

where, $\Delta\phi_e^0$ = Standard electrode potential.

Combination of Eqs. (2.4) and (2.5) leads to

$$0 = -zF\Delta\phi_e^0 - RT\ln a_{M^{z+}} + zF\Delta\phi_e$$

$$\Rightarrow \Delta\phi_e = \Delta\phi_e^0 + (RT/zF) \ln a_{M^{z+}} \dots\dots\dots(2.6)$$

Equation (2.6), known as Nernst equation, gives the effect of concentration on electrode potential.

From the moment that a current flows through an electrode, the electrode acquires a potential different from the reversible equilibrium potential. It is well to note here that equilibrium means dynamic equilibrium and that although no net current flows through the electrode, oxidation and reduction reactions will take place simultaneously, such that the oxidation current density i_{ox} is equal in magnitude to the reduction current density i_{red} . Both are, at equilibrium, equal to the so-called exchange current density and the equilibrium potential across the electrode is $\Delta\phi_e$.

In order to realize electrodeposition at a cathode, a net current $i = (i_{ox} - i_{red}) < 0$ has to flow through the cathode. Therefore the potential $\Delta\phi$ over the electrode interface has to deviate from $\Delta\phi_e$. This deviation is called the activation overpotential (η).

$$\text{Hence } \Delta\phi = \Delta\phi_e + \eta$$

The term activation refers to the fact that the electrode reaction is a kinetic process, in which substances must acquire a certain activation energy before they can jump through the electrode interface. Deviation from the equilibrium potential is called polarization.

As a result of the electrode reaction, the ionic concentration tends to change in the vicinity of the electrode, resulting in a concentration overpotential η_{con} . For a reduction reaction at the cathode, for example, the concentration of positive ions is lowered, and the equilibrium potential shifts according to the Nernst equation. If, as a result of an increasing cathodic polarization, the reduction current density is increased, positive ions have to be brought to the cathode surface faster and faster. This can occur by

- i) mitigation under influence of the electrical field
- ii) diffusion due to the created concentration differences
- iii) natural or forced convection.

Another component is the crystallization overpotential (η_{cr}) originating from difficulties encountered with nucleation and growth. Minute concentrations of foreign substances can drastically increase the crystallization overpotential, and thus effectively slow down the electrodeposition process. The global electrode overpotential is, now

$$\eta_{\text{tot}} = \eta + \eta_{\text{con}} + \eta_{\text{cr}} \quad \dots\dots\dots(2.7)$$

An electrodeposition cell contains two electrodes: a cathode and an anode. Both contribute to the total cell potential according to equation (2-7).

In addition there is the resistance of the electrolyte leading to a potential IR , and various other resistances in the cell circuit creating a potential E_R . The total cell potential is then

$$E_{\text{tot}} = E_{\text{rev}} + \eta^{\text{antot}} + \eta^{\text{catot}} + IR + E_R$$

The practical cell potential is therefore sometimes much higher than the reversible cell potential calculated from purely thermodynamic considerations.

2.2 Principles of Alloy Electrodeposition

2.2.1 Introduction

Generally the procedure for depositing an alloy is almost the same as that for a single metal - a current is passed from electrodes through a solution and then metal deposits upon the cathode. However, the problem of finding conditions for depositing a given alloy in the form of a sound, strong homogeneous coating is not as easily solved as for a single metal. The simultaneous deposition of two or more metals without regard to the physical nature of the deposit is a relatively simple matter, for it is necessary only to electrolyze a bath of the mixed metallic salts at a sufficiently high current density. Unfortunately, the deposits so obtained are usually loose, spongy, nonadherent masses, contaminated with basic

inclusions, and are not the type of deposit of interest. Thus the use of a high current density is not a means of solving the problem of alloy deposition.

A preliminary and rather obvious requirement for codepositing two or more metals from aqueous solution is that at least one of the metals be individually capable of being deposited from aqueous solution.

The most important practical consideration involved in the codeposition of two metals is that their deposition potentials be fairly close together. The importance of this consideration follows from the well known fact that the more noble metal deposits preferentially, frequently to the complete exclusion of the less noble metal. To simultaneously codeposit two metals, conditions must be such that the more negative potential of the less noble metal can be attained without employing an excessive current density. Hence, the need for having the potentials of the two metals close together.

2.2.2 Static Potentials and Electrodeposition of Alloys

The table of standard electrode potentials, Table 2.1 may serve as a rough but not too reliable guide for deciding if two metals may be co-deposited from a simple salt solution. The data in Table 2.1 apply only to very specific conditions and are, therefore, of limited applicability. This must be further emphasized before proceeding with a discussion of their value for predicting the probability of co-deposition of two metals. The electrode potentials in Table 2.1 apply

only to the equilibrium potentials of the metals in a solution of their simplest ions and are just about the most positive (most noble) potentials at which the metals can be deposited. In actual deposition, because of polarization, the deposition potentials are more negative than the standard potentials.

The deduction from a table of electrode potentials of the probability of, and the conditions for, depositing a single metals is not straightforward. As an example, if one were to make a naive interpretation of Table 2.1 without regard to practical considerations, one would come to the conclusion that metals with electrode potentials more negative than hydrogen could not be deposited from aqueous solution because hydrogen would deposit at a more positive (more noble) potential. Actually, hydrogen deposits at a much more negative potential than its equilibrium value on many kinds of metal electrodes (the phenomenon of hydrogen overvoltage), and, consequently, the potentials of some of these metals can be attained in aqueous solution without excessive discharge of hydrogen. Even manganese with an equilibrium potential of -1.18 V can be deposited from aqueous solution by virtue of its hydrogen overvoltage. The existence of this phenomenon is fortunate for electrodepositions, because the majority of the metals in which electroplates are interested have potentials less noble than that of hydrogen. Another example of the opposite kind concerns the metals vanadium, molybdenum, germanium and tungsten which have the following electrode potentials, respectively: -0.253 , -0.2 , -0.15 and -0.09 volt. According to Table 2.1, these metals ought to be more readily depositable from aqueous solution than cobalt with a potential of -0.277 volt.

Table 2.1 Standard Electrode Potentials (E^0)

Electrode Reaction	E^0 (Volts),250°C
$\text{Na} = \text{Na}^+ + e$	- 2.712
$\text{Mg} = \text{Mg}^{+2} + 2e$	- 2.340
$\text{Al} = \text{Al}^{+3} + 3e$	- 1.670
$\text{Mn} = \text{Mn}^{+2} + 2e$	- 1.180
$\text{Zn} = \text{Zn}^{+2} + 2e$	- 0.762
$\text{Co} = \text{Co}^{+2} + 2e$	- 0.277
$\text{V} = \text{V}^{+2} + 2e$	- 0.253
$\text{Ni} = \text{Ni}^{+2} + 2e$	- 0.250
$\text{Mo} = \text{Mo}^{+3} + 3e$	- 0.200
$\text{Ge} = \text{Ge}^{+4} + 4e$	- 0.150
$\text{Sn} = \text{Sn}^{+2} + 2e$	- 0.136
$\text{Pb} = \text{Pb}^{+2} + 2e$	- 0.126
$\text{W} = \text{W}^{+6} + 6e$	- 0.090
$\text{H}_2 = 2\text{H}^+ + 2e$	0.000
$\text{Bi} = \text{Bi}^{+3} + 3e$	+ 0.320
$\text{Cu} = \text{Cu}^{+2} + 2e$	+ 0.345
$\text{Cu} = \text{Cu}^+ + e$	+ 0.522
$\text{Ag} = \text{Ag}^+ + e$	+ 0.800
$\text{Pt} = \text{Pt}^{+2} + 2e$	+ 1.200
$\text{Au} = \text{Au}^{+3} + 3e$	+ 1.420
$\text{Au} = \text{Au}^+ + e$	+ 1.620

However, none of these metals have been deposited from aqueous solution the pure state, whereas cobalt is readily deposited. We do not know why these metals do not deposit but the situation is not unique. The nonoccurrence of reactions which are thermodynamically possible is quite common in chemistry. This means that other requirements must be satisfied as well as the energetics of the process.

To sum up the discussion of electrode potentials, we see, on one hand, that many metals can be deposited, which would not be expected to deposit on the basis of equilibrium potentials; and on the other hand, that metals which are theoretically capable of being deposited have not been deposited from aqueous solution.

Despite these inconsistencies, the table of electrode potential can be utilized to derive some conclusions regarding alloy deposition from acid solution of simple ions. Metals which are close together in Table 2.1 should in general be more readily codeposited than metals which are widely separated. As a rough guide, reasonably satisfactory co-deposition will occur if the static potentials of the metals are not over 0.2 volt apart. However, exceptions may be noted; for example, Zn and Ni may be co-deposited from a simple salt bath, although their electrode potentials are about 0.5 volt apart. An exception of the opposite kind occurs with some of the noble metals. For example, silver and palladium do not readily co-deposit to yield good alloys although their potentials are very close together. This discussion shows that the predictions concerning alloy deposition from electrode potentials alone are not wholly

reliable and may be misleading because many unpredictable specific effects occur with each pair of metals.

The potential of metal dipping into a solution of its ions at unit activity is the standard electrode potential of the metal, E^0 . When the activity of the ions is not unity the static potential E_S is given by

$$E_S = E^0 - (RT/nF) \ln a \quad \dots\dots\dots(2.8)$$

where, R = Gas constant

T = Absolute temperature

n = Valence change in the reaction metal-metal ion

F = The Faraday's constant

a = Activity of metal ion

Equation (2.8) represents the equilibrium reversible conditions. Irreversible factors (concentration, polarization, overvoltage etc.) however enter in if current is passed so that metal deposits from a solution. The actual deposition potential is then given by

$$E_D = E_S + P$$

Where P is a measure of irreversible effects, i.e. the additional potential that has to be provided to keep the reaction going at the required speed.

To codeposit two metals, the deposit potential of the two metals should be nearly equal. The following conditions should, therefore, be satisfied for co-deposition of alloys:

$$E_D' = E_D''$$

$$\Rightarrow E_S' + P' = E_S'' + P''$$

$$\Rightarrow E^{0'} - (RT/n'F) \ln a' + P' = E^{0''} - (RT/n''F) \ln a'' + P'' \dots\dots\dots(2.9)$$

where E_D' , $E^{0'}$ and a' are deposition potential, electrode potential and activity of one metal respectively. Similarly E_D'' , $E^{0''}$ and a'' are deposition potential, electrode potential and activity of the other metal respectively desired to be co-deposited. In equation (2.9), R and F are fixed. T is constant in any given case. Thus, equation (2.9) can be satisfied only in the following ways:

i) Metals placed close together in electro-chemical series: If the two metals to be co-deposited are already close together in the electro-chemical series, $E^{0'}$ may become equal to $E^{0''}$. A good example is Sn-Pb alloy.

$$E^0 \text{ for Sn} = -0.14V \quad E^0 \text{ for Pb} = -0.13V$$

These are so close together that Sn and Pb may be co-deposited from solutions of their simple salts with no difficulty. Generally metals whose E^0 values differ by less than 0.2V can be co-deposited from simple salt solutions because polarization may bring the potential values closer together.

ii) Adjustment of $a^{0'}$ and $a^{0''}$: If $E^{0'}$ does not equal $E^{0''}$ the activity $a^{0'}$ and $a^{0''}$ must be adjusted to make the deposition potential equal.

The Nernst equation [$E = E^0 + (0.059/n) \log a_{M^{n+}}$] relates electrode potential to metal ion activity and consideration of this equation shows that a reduction in ion activity corresponds to a potential shift in the negative direction and conversely an increase in ion activity moves the potential to more positive values. For a monovalent ion the shift is 0.059 V per order of magnitude change in activity. A well-known means of reducing the ion activity of the more noble metal is the addition of complexing agents. As an example let us consider the alloy deposition of Ag-Pb alloys.

The E^0 values are: Ag = + 0.789; Pb = 0.13

The potentials may be equalized if the more noble metal is complexed (Ag) and the less noble metal maintained uncomplexed. Only Ag forms a cyanide complex and from the Nernst equation we can calculate the activity of Ag ions required to lower the potentials to - 0.13 V.

$$- 0.13 = + 0.789 + 0.059 \log [Ag^+]$$

$$\Rightarrow [Ag^+] = 10^{-16} M.$$

This can be achieved by cyanide complexing provided an excess of cyanide ion is maintained.

The most common complexants are cyanide, halide and amphoteric oxides like stannate, but amines, citrates, tartarates, etc. find application.

2.2.3 Criteria for Electrodeposition of Alloy

The six principles of alloy deposition are

- i) If an alloy plating bath, which is in continuous operation, is replenished with two metals in a constant ratio, M/N (for example, by adding metallic salts or by the use of soluble anodes), the ratio of the metals in the deposit will approach and ultimately take on the value M/N.
- ii) An increase in the metal-percentage (or ratio) of a parent metal in an alloy plating bath results in an increase in its percentage (or ratio) in the deposit.
- iii) In alloy deposition, the ratio of the concentration of the more readily depositable metal to the other is smaller at the cathode-solution interface than in the body of the bath.
- iv) In the deposition of alloys from the normal alloy plating systems, the most fundamental mechanism is the tendency of the concentrations of the metal ions at the cathode-solution interface to

approach mutual equilibrium with respect to the two parent metals. Both principles iii) and iv) lead to the relation.

$$C_m/C_n < C_m^0/C_n^0$$

Where, C_m = Concentration of more readily depositable metal at the cathode-solution interface.

C_n = Concentration of less readily depositable metal at the cathode-solution interface.

C_m^0 = Concentration of more readily depositable metal in the body of the bath.

C_n^0 = Concentration of less readily depositable metal in the body of the bath.

v) A variation in a plating condition that brings closer together the potentials for the deposition of the parent metals separately — that is, decreases the interval of potential between them increases the percentage of the less noble metal in the electrodeposited alloy and vice-versa.

vi) In depositing alloys in which the content of the less noble metal increase with current density, the operating conditions for obtaining the more constant composition of deposit are: (a) constant potential if the uncontrollable variable affect the potentials of the more noble metal and (b) constant current density if the uncontrollable variables affect the potential of the less noble metal. Conditions (a) and (b) are interchanged if the content of the noble metal decreases with current density.

2.3 Electrodeposition of Zn-alloy

From the electronegative potential of zinc (-0.76 volts), it might be expected that zinc could not be electrodeposited from aqueous solution. But in fact the high overpotential of hydrogen on most substrates does permit such deposition. Further, the general considerations for codeposition is that the standard electrode potentials of those metals be fairly close together. But the standard electrode potential of zinc, $E = -0.76$ volts, is far from other metals, particularly from iron group metals (Ni: -0.25 volts; Co: -0.28 volt; and Fe: -0.44 volt) and one would not expect zinc to codeposit readily with the iron group metals. Therefore it is surprising not only that codeposition does occur, but also that zinc deposits preferentially under most conditions of plating.

Since zinc codeposits readily with the iron group metals, a large amount of work has been done for depositing zinc-alloys and most of those for Zn-Ni alloys.

Various baths have been used for depositing Zn-Ni alloys, which are classified as acid and alkaline baths. Different baths which are generally used are as follows:

A Electrodeposition of Zn-Ni Alloys from Chloride or Sulphate Solutions

Most of the studies of electrodeposition of Zn-Ni alloys were made with acid baths containing simple sulphate or chloride salts of

the metals. The composition of the various baths which have been used for depositing Zn-Ni alloys as described in the literature are listed in Table 2.2 They are readily prepared and of simple composition.

Though bath composition is an important factor, to get Zn-Ni alloy deposits of satisfactory physical properties the plating conditions are of great importance. Since the optimum pH for operating the simple Zn-Ni baths is about 2, the buffering of the bath is important. Borric acid was used in some baths, but seems too weak an acid to be of use. Some investigators used weak organic acid as well as dilute (0.01N) H_2SO_4 or HCl. The bath pH range should be 2-4. The best plating conditions are moderate current densities at elevated temperature.

No detailed study has been made of anodes for Zn-Ni plating. Most of the investigators used soluble electrode. Zinc is widely used for this purpose^{3,4}. A dual anode system consisting of pure zinc and nickel is also employed⁵.

The most serious disadvantage of using insoluble anodes are :
i) the concentration of the depositable metal decreases; ii) the pH of the bath decreases.

General acid sulphate baths yields black, powdery deposits. Addition agents may improve the appearance of the deposits. Several brightner systems have been used to make the deposits smooth, bright and better corrosion resistance. For example organic

additive phenolic derivative³ Veratraldehyde and Teepol⁵, ammonium chloride⁴ have been used to brighten the deposits.

Temperature of the bath are also adjusted because the nickel content of the deposits depends on the bath temperature.

B. Electrodeposition of Zn-Ni Alloys from a Sulphamate Bath

The composition of a typical sulphamate bath is given in Table-2.2, bath no. 8. The performance of the bath should resemble that of simple sulphate or chloride bath. The variables that were found⁵ to have the largest effect on the composition of deposit were temperature and pH.

C. Electrodeposition of Zn-Ni Alloys from Ammoniacal Baths

Comparatively less work has been done on the ammoniacal bath. The compositions of typical bath is given in Table 2.2, bath no. 9. This bath is operated at a low current density.

The alloy obtained from the ammoniacal bath were sounder than those deposited from the acid baths, but they were dark in color. The main interest in the ammoniacal bath is that the alloy deposition was the anomalous type, inasmuch as zinc deposited preferentially.

D. Electrodeposition of Zn-Ni Alloys from the Pyrophosphate Bath

Pyrophosphate bath is also used to electrodeposit Zn-Ni alloy. The composition of typical plating bath is given in Table - 2.2, bath No. 10. The molar concentration of pyrophosphate ion, P_2O_7 , was 2.5 times the total metal concentration in moles or on a weight basis, 7 times the total metal content of the bath. The deposits varied in color from light to dark gray, but in the presence of addition agents some bright deposits were obtained. The deposition of the Zn-Ni alloys is mainly of the anomalous type.

The effects of pH of the bath, pyrophosphate concentration, or total metal content had only minor effects on the composition of the deposit. The nickel content of the alloy from this bath increased with elevation of temperature and with agitation of the plating baths⁶.

Table 2.2 A summary of commonly used Zn-Ni alloy plating baths.

Bath	Composition of bath						Reference
	Ni-Salt		Zn-salt		Other additions		
	Formula	Conc gm/l	Formula	Conc gm/l	Formula	Conc. gm/l	
1.	$\text{NiSO}_4 \cdot 7\text{H}_2\text{O}$	250	$\text{ZnSO}_4 \cdot 7\text{H}_2\text{O}$	287	H_3BO_3	30	7
2.	$\text{NiSO}_4 \cdot 7\text{H}_2\text{O}$	265	$\text{ZnSO}_4 \cdot 7\text{H}_2\text{O}$	150	Na_2SO_4	150	4
3.	$\text{NiSO}_4 \cdot 7\text{H}_2\text{O}$	200	$\text{ZnSO}_4 \cdot 7\text{H}_2\text{O}$	10	H_3BO_3	35	4
4.	$\text{NiCl}_2 \cdot 6\text{H}_2\text{O}$	217	ZnCl_2	78	CH_3COOH	22	4
5.	$\text{NiCl}_2 \cdot 6\text{H}_2\text{O}$	234.8	ZnCl_2	135	H_3BO_3	30	3
					NaCl	155	
6.	$\text{NiCl}_2 \cdot 6\text{H}_2\text{O}$	60	ZnCl_2	100	KCl	149	
7.	$\text{NiCl}_2 \cdot 6\text{H}_2\text{O}$	240	$\text{ZnSO}_4 \cdot 7\text{H}_2\text{O}$	260	CH_3COOH	30ml	8
8.	Ni-sulphamate	65	$\text{ZnSO}_4 \cdot 7\text{H}_2\text{O}$	200	H_3BO_3	30	5
					Na-citrate	60	
9.	$\text{NiSO}_4 (\text{NH}_4)_2\text{SO}_4 \cdot 6\text{H}_2\text{O}$	15	$\text{ZnSO}_4 \cdot 7\text{H}_2\text{O}$	11	Aqua ammonia	60ml	11
10.	$\text{NiCl}_2 \cdot 6\text{H}_2\text{O}$	71	$\text{Zn}_2\text{P}_2\text{O}_7$	153	$\text{K}_4\text{P}_2\text{O}_7 \cdot 3\text{H}_2\text{O}$	192	9

2.3.1 Effect of Plating Variables on the Composition of the Deposit

2.3.1.1 Effect of Bath Composition

In Zn-Ni alloy deposition, zinc is the most readily deposited metal and alloy deposition is of the anomalous type, as the percentage of zinc, the less noble metal, in the deposit is always higher than its percentage in solution³.

When the percentage of nickel in the deposits and in the solution are related, linear dependencies are obtained for all the deposition baths considered [Fig. 2.1].

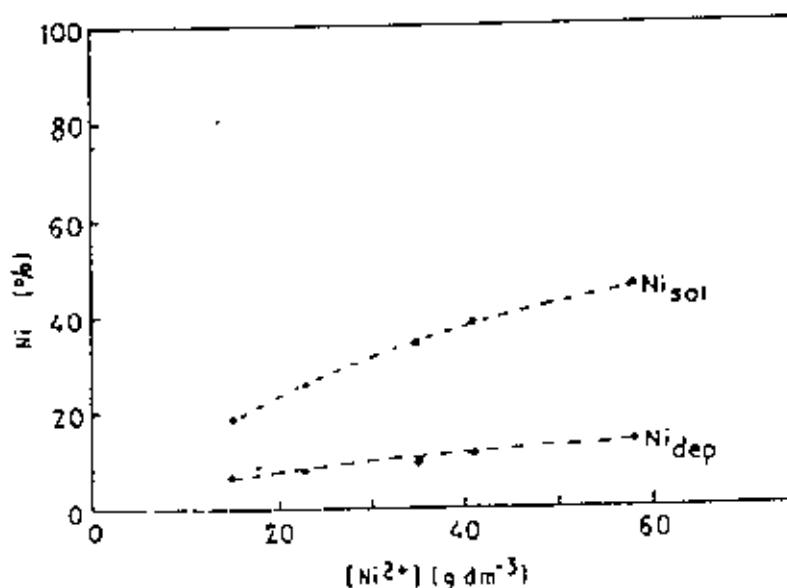


Fig. 2.1 The percentage of nickel in the alloys deposited from the baths.

As modified Roehl bath, (ZnCl₂ 0.57M, NiCl₂ 0.92M and acetic acid 0.366M) the higher nickel-to-total metal ratio, consistently produces higher nickel composition in the deposit¹⁰.

Fig. 2.2 comes from the work of Schoch and Hirsch¹¹. Although the total metal content of their baths varied widely, this does not vitiate the relation between the metal ratio of bath and the deposit. AB is the composition reference line.

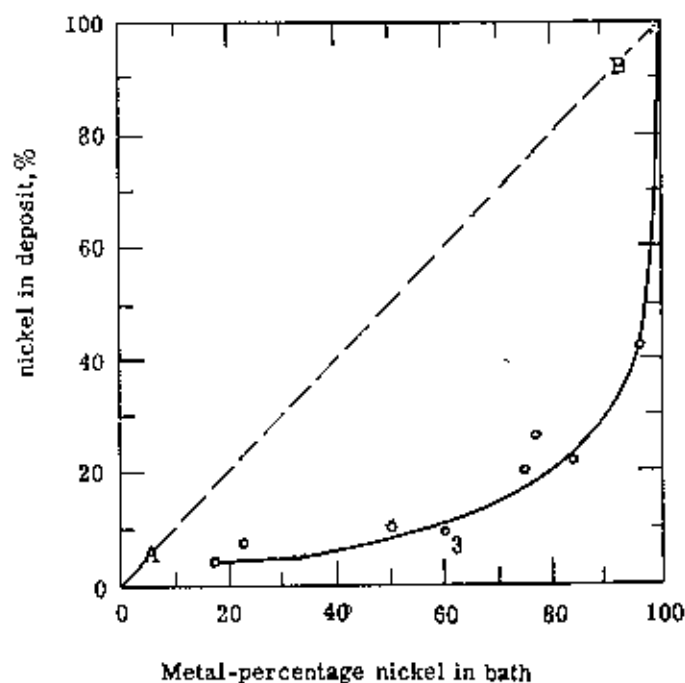


Fig. 2.2 Relation between the composition of deposit and of the bath in Zn-Ni alloy deposition.

2.3.1.2 Effect of current density

The best pedagogic approach to the rather complicated relations between alloy composition and current density in anomalous codeposition is to first study a curve which exhibits most of the various types of relations. In Fig. 2.3, curve 5 represents the deposition of iron-zinc alloys from an acid sulfate bath at 90°C.

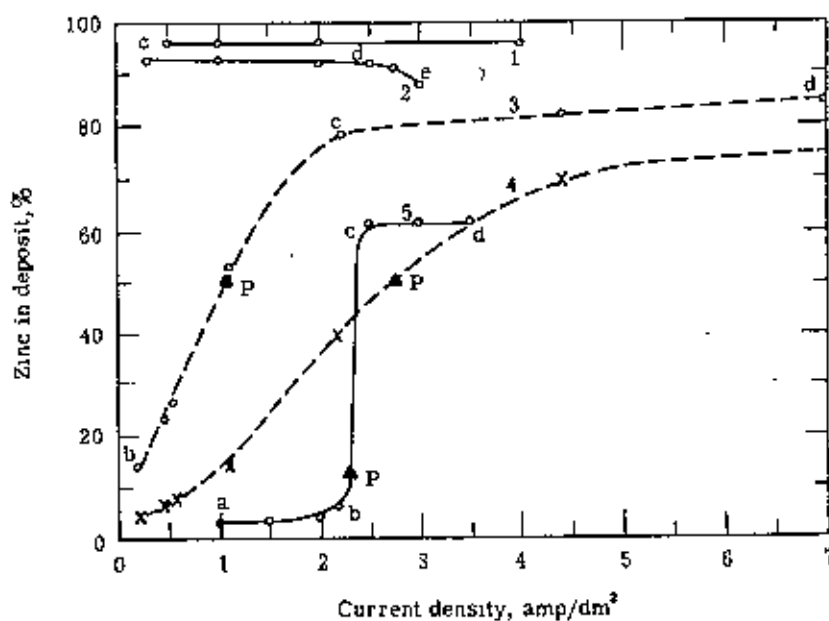


Fig. 2.3 Relation between alloy composition and current density in anomalous codeposition of zinc with iron or nickel. Points P represent the metal-percentages of zinc in the baths

The data are from the work of von Escher and others¹². The point P indicates the metal-percentage zinc in the bath, which is 11.5%. The curve consists of three branches. In the low current density region, from a to b, the codeposition appears to be of the normal type, that is, the deposit contains a smaller content of the less noble metal, zinc, than corresponds to the metal-percentage zinc, P, in the bath, and with increasing current density the content of zinc in the deposit increases. However, instead of approaching a limit of 11.5% zinc, with increasing current density, as would be the case with regular codeposition, the deposit rapidly increase in zinc content and above 2.5 amp/dm² contains much more zinc than corresponds to the metal-percentage zinc in the bath.

The transition of the zinc content of the deposit from a value well below, to a value well above, the metal-percentage zinc of the bath occurs over a rather small range of current density (branch bc). The current density at the point P where the per cent zinc in the deposit just equals the metal-percentage zinc of the bath will be referred to as the "transition current density." The point P is not an equilibrium point and should not be confused with apparently similar points on curves representing equilibrium codeposition where the bath and the alloy composition are the same.

The third branch of curve 5, from c to d, exhibits little change in alloy composition with current density. Since zinc is depositing preferentially, the cathode film must be relatively more depleted in zinc than in iron; consequently, in the absence of agitation caused by hydrogen evolution, the deposition should be under diffusion control, and the zinc content of the deposit should tend down-wards at still higher current density.

The other curves of Fig. 2.3 exhibit only one or two of the four types of relations between composition and current density. For example, curves 3 and 4 for the deposition of nickel-zinc alloys from an acid chloride bath¹³ show only two branches. The low current density region from a to b is missing. Curves 1 and 2 taken from the data of Schoch and Hirsch¹¹ show only the branch cd and de of the composition-current curve. Apparently, the other branches, and also the transition current density, lie at very low current densities. It is possible that these branches, a to c, could have been obtained by plating at low current densities, but it is likely that the attempt

would be vitiated by practical considerations, such as very low cathode current efficiencies or the deposition of mossy deposits.

The effect of cathodic current density on the deposits as studied by means of electroplating experiments at different current densities between 15.6 and 62.5 mA/cm², keeping all other plating conditions constant. As seen in Fig. 2.4 alloy composition is not affected significantly by current density variation³.

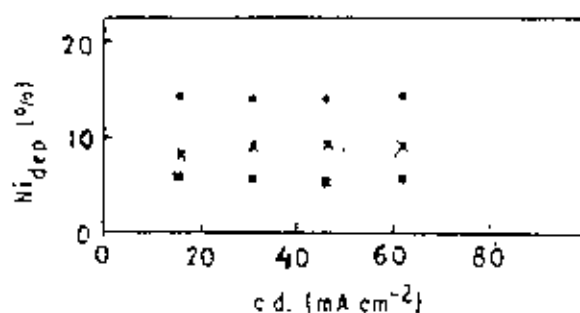


Fig. 2.4 Effect of current density (c.d.) on the percentage of nickel in electrodeposited Zn-Ni alloys from baths containing the following amounts of nickel: (■) 18.8, (x) 35.0 and (•) 47.2% of Ni²⁺. For $t = 25^{\circ}\text{C}$.

2.3.1.3 Effect of Temperature

In the deposition of Zn-Ni alloys the main effect of raising the temperature of the plating bath was to some extent relieve the anomalous nature of the codeposition, with the result that the zinc content of the deposit diminished. The deposition potentials of the metals usually become more noble with increase in temperature because polarization is decreased. The reduction of polarization which occurs on raising the temperature of the plating bath should be larger for nickel, the more noble metal, and the deposition of the latter should be favored to a larger extent than that of Zn, the less noble metal. At current densities less than 0.3 A cm^{-2} the effect of increasing the temperature at a given current is to increase the nickel content seen in Fig. 2.5 for modified Rochl bath¹⁰.

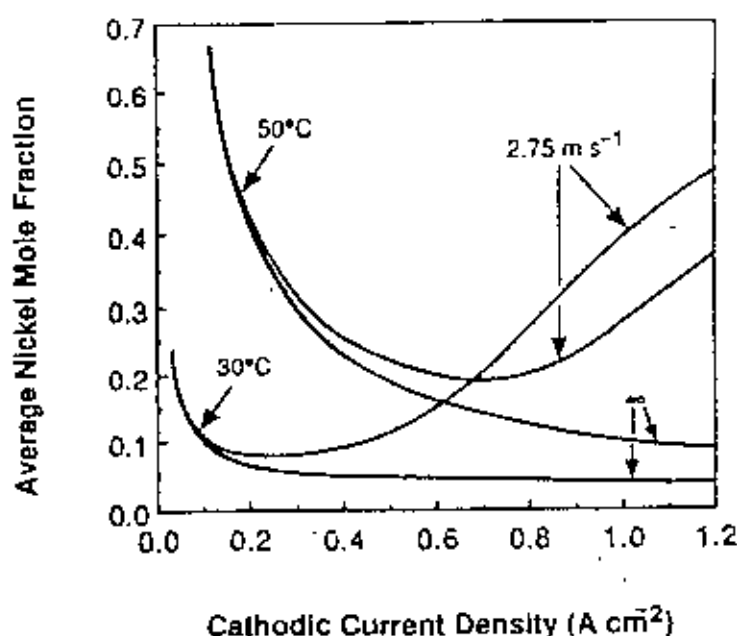


Fig. 2.5 Effect of the temperature on the nickel content of the alloy.

2.3.1.4 Effect of pH

Bath pH variation within the narrow acidic region of 1.0-4.0 did not affect the coating composition significantly. However, coating deformability was adversely affected if bath pH exceeded 2.5. At pH values less than 1.0, cathode current efficiency decreased rapidly owing to excessive hydrogen evolution⁴.

2.4 Corrosion testing

2.4.1 Introduction

Zinc protects steel galvanically or “sacrificially” that is in the corrosion couple set up between the substrate steel and the coating metal, the latter is normally anodic to the substrate and corrodes preferentially. The substrate steel, being the cathode in the couple is protected as long as there is any coating left in the immediate vicinity.

Zn-Ni alloy coating offers better corrosion protection, both barrier and galvanic to the underlying steel substrate. Many types of corrosion tests are made for comparison of Zn and Zn-Ni alloy coatings.

2.4.2 Purpose of Corrosion Testing

Perhaps the main justifications for corrosion testing are

1. Evaluation and selection of materials for a specific environment or a given definite application. This could be a new or modified plant or process where previous operating history is not available. It could involve an old plant or process that is to be replaced or expanded with more economical materials of construction or materials that would exhibit less contamination of product, improved safety, more convenient design and fabrication, or substitution of less strategic materials.

2. Evaluation of new or old metals or alloys to determine the environments in which they are suitable. Much of this type of work is done by producers and vendors of materials. The information obtained aids in the selection of materials to be tested for a specific application. Inclusion of tests on other materials which are known to be in commercial use in these environments permits helpful comparisons. In the case of new metals and alloys, the data obtained provide information concerning possible applications. This category could also include the effects of changes in environment—such as additions of inhibitors or deaeration—on corrosion of metals and alloys.

3. Control of corrosion resistance of the material or corrosiveness of the environment. These are usually routine tests to check the quality of the material. The Huey test (boiling 65% nitric acid) is used to check the heat treatment of stainless steels.

Another example is the salt-spray test, where specimens are exposed in a box or cabinet containing a spray or fog of seawater or salt water. This type of test is often used for checking or evaluating paints and electroplated parts. These tests may not be directly related to the intended services but are sometimes incorporated in specifications as acceptance tests. In some cases periodic testing is required to determine changes in the aggressiveness of the environment because of operating changes such as temperatures, process raw materials, changes in concentrations of solutions, or other changes that are often regarded as insignificant from the corrosion standpoint by operating personnel. Probe techniques, described later, are also very helpful here.

4. Study of the mechanisms of corrosion or other research and development purposes. These tests usually involve specialized techniques, precise measurements, and very close control.

2.4.3 Surface Preparation for Corrosion Testing

Ideally the surface of the test specimen should be identical with the surface of the actual equipment to be used in the plant. However, this is usually impossible because the surfaces of commercial metals and alloys vary as produced and as fabricated. The degree of scaling or amounts of oxide on the equipment varies and also the conditions of other surface contaminants. Because of this situation and because the determination of the corrosion resistance of the metal or alloy itself is of primary importance in most cases, a clean metal surface is usually used. A standard surface condition is also desirable and necessary in order to facilitate comparison with results of others.

A common and widely used surface finish is produced by polishing with No. 120 abrasive cloth or paper or its approximate equivalent. This is not a smooth surface, but it is not rough, and it can be readily produced. Prior treatments such as machining, grinding, or polishing with a coarse abrasive may be necessary if the specimen surface is very rough or heavily scaled. All these operations should be made so that excessive heating of the specimen is avoided. A good general rule is that the specimen could at all times be held by the naked hand. The 120 finish usually removes sufficient metal to get below any variations (such as decarburization or carburization) in the original metal surface.

Clean polishing belts or papers should be used to avoid contamination of the metal surface, particularly when widely dissimilar metals are being polished. For example, a belt used to polish steel should not then be used to polish brass or vice versa. Particles of one metal would be imbedded in the other and erroneous results obtained.

A smoother finish may be required in certain cases such as actual equipment that requires a highly polished surface or sometimes where extremely low rates of corrosion are anticipated.

Quite often test specimens are made by shearing from a thin plate or sheet. The edges must be machined, filed, or ground to remove the severely cold-worked metal and subsequently finished similarly to the remainder of the specimen. The edges and corners of the specimens should be slightly beveled or rounded to facilitate polishing.

Soft metals such as lead would tend to smear if polished on an emery belt. Rubbing with a hard eraser until a bright surface is obtained is a recommended procedure for lead and lead alloys. A sharp blade is sometimes used to shave or prepare lead specimens. The soft metals also present the problem of the abrasive being imbedded in the surface. Scrubbing with pumice powder and other fine abrasives is sometimes used on magnesium, aluminum, and their alloys. electrolytic polishing is occasionally used for research work but is not generally recommended for plant tests.

Chemical treatments or passivating pretreatments for stainless steels and alloys are sometimes used but are not recommended because false and misleading results might be obtained. A passivity treatment may result in good corrosion resistance during testing but may not be effective during actual service of the equipment. In other words, a material should not be used in service if its corrosion resistance depends upon an artificial passivation treatment. Natural passivity effects would show up during tests to determine the effect of time on corrosion. Chemical treatments are utilized to decontaminate metal surfaces and serve a useful purpose here.

2.4.4 Measuring and Weighing

After surface preparation the specimens should be carefully measured to permit calculation of the surface area. Since area enters in the formula for calculating the corrosion rate, the results can be no more accurate than the accuracy of measurement of the surface area. The original area is used to calculate the corrosion rate throughout the test. If the dimensions of the specimen change appreciably during the test, the error introduced is not important because the material is probably corroding at too fast a rate for its practical use.

After measuring, the specimen is degreased by washing in a suitable solvent such as acetone, dried, and weighted to nearest 0.1 mg (for small specimens). The specimen should be exposed to the corrosion environment immediately or stored in a desiccator, particularly if the material is not corrosion-resistant to the atmosphere. Direct handling of the specimens is undesirable.

2.4.5 Exposure Techniques

A variety of methods are utilized for supporting specimens for exposure in the laboratory or in the plant. The important considerations are: (1) The corrosive should have easy access to the specimen; (2) the supports should not fail during the test; (3) specimens should be insulated or isolated electrically from contact with another metal unless galvanic effects are intended; (4) the specimen should be properly positioned if effects of complete immersion, partial immersion, or vapor phase are being studied;

and(5) for plant tests, the specimens should be as readily accessible as possible.

2.4.6 Standard Expressions for Corrosion Rate

In most cases, aside from contamination problems, the primary concern is the life (usually life in years) of the equipment involved. A good corrosion rate expression should involve (1) familiar units, (2) easy calculation with minimum opportunity for error, (3) ready conversion to life in years, (4) penetration, and (5) whole numbers without cumbersome decimals.

Mils per year is now widely used. The formula for calculating this rate is

$$\text{Mils per year} = \frac{534W}{DAT}$$

where, W = weight loss, mg

D = density of specimen, g/cm³

A = area of specimen, sq. in.

T = exposure time, hr.

2.4.7 Classification of Corrosion Tests

Corrosion testing is divided into four types of classifications: (1) laboratory tests, including acceptance or qualifying tests: (2) pilot-plant or semiworks tests: (3) plant or actual service tests: and (4) field tests. The last two could be combined, but to avoid confusion in terminology the following distinction is made: the third involves

tests in a particular service or a given plant, whereas the fourth involves field tests designed to obtain more general information. Examples of field tests are atmospheric exposure of a large number of specimens in racks at one or more geographical locations and similar tests in soils or seawater.

Laboratory tests are characterized by small specimens and small volumes of solutions, and actual conditions are simulated insofar as conveniently possible. The best that can be done in this regard is the use of actual plant solutions or environment. Laboratory tests serve a most useful function as screening tests to determine which materials warrant further investigation. Sometimes plants are built based primarily on laboratory tests, but results could be catastrophic and sometimes are.

2.4.8.1 Salt Water Immersion Test

Salt solution immersion test is done for studying the corrosion behaviors of coatings. 3 wt.% NaCl solution is generally used for this purpose. The substrate of fixed area exposed is immersed in that solution and is measured by the time taken to form red rust on it⁴.

The neutral salt-spray tests are commonly used for evaluating the corrosion behavior of Zn-Ni alloy plating of various composition and the performance compared with that of pure zinc⁵. The corrosion resistance of the electroplates is evaluated by observing the propagation of both white and red rust formed on deposits 10 μm thick, which were tested in 5% NaCl solution spray environment¹.

2.4.8.2 Hot Water-Immersion Test

The hot water immersion test was one of the earliest accelerated corrosion tests and was used to detect the porosity in tin plating. It is now recognized as an accepted test for nickel and other coatings on steel or iron for industrial chemical equipment.

The hot-water test consists of immersion in water at $180 \pm 5\text{F}$ with aeration for 1 to 4 hr. The appearance of six rust spots per square foot of surface has been used as a basis for rejection for nickel-plated coatings for some applications. A temperature of 180 F gives the maximum corrosion of steel in aerated water as, for example, when testing nickel coatings on steel. The optimum temperature will vary for different base metals. For example 116 F has been used for nickel coatings or chemical conversion coatings on zinc-base die castings.

This test disclosed discontinuities in nickel coatings which would result in rapid failure of nickel-plated chemical equipment. It also determines the degree of protection of chemical conversion coatings on zinc-base die castings or zinc coatings against formation of white corrosion products.

2.4.9 Electrochemical Test

2.4.9.1 Polarization Techniques for Estimating Corrosion Current

The rates of both cathodic and anodic reaction usually follow Tafel behavior, i.e.,

$$E = a + b \log i \quad (2.10)$$

Where E is the electrode potential of the specimen, i is the current density of the electrochemical reaction, and a and b are constants.

The "b" constant in this equation is often referred to as the Tafel slope and is usually expressed in mV/decade(dec). The corrosion current can be estimated if the electrochemical corrosion processes follow this Tafel behavior. The net current density on the specimen is related to the current densities of the electrochemical reactions occurring on the specimen surface by the following equation:

$$i_{\text{net}} = i_{\text{anode}} - i_{\text{cathode}} \quad (2.11)$$

The exponential behavior of current density with potential means that the anodic contribution to the net current density can generally be ignored if the specimen potential is 50 mV more negative than the open circuit value, while the cathodic contribution is usually negligible at potentials 50 mV more positive than the open circuit value. These relationships are shown diagrammatically in Figure 2.6¹⁴.

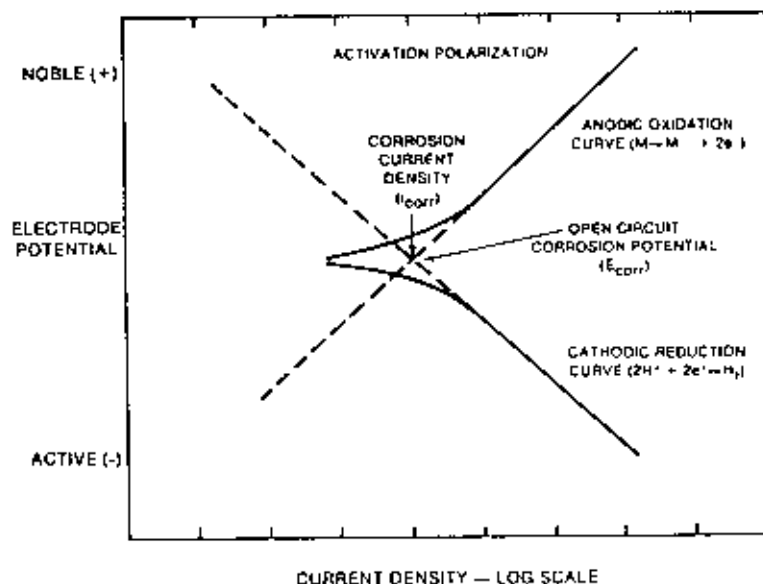


Fig. 2.6 Schematic cathodic and anodic polarization curve

Based on these observations, several techniques can be used to estimate corrosion currents the specimen can be polarized to potentials at least 50 mV more negative than the open circuit corrosion potential, and sufficient data points taken to obtain reliable Tafel line. Then the current density data can be extrapolated back to corrosion potential using a semilogarithmic plot to obtain the corrosion current density value. The second technique is analogous to the first in that the specimen can be polarized anodically to potentials greater than 50 mV more positive than the corrosion potential, and the same process repeated. The third technique requires that both cathodic and anodic polarizations be carried out as described above, and the corrosion current is obtained at the intersection of the anodic and cathodic extrapolated lines. These three techniques are illustrated in Fig. 2.7.

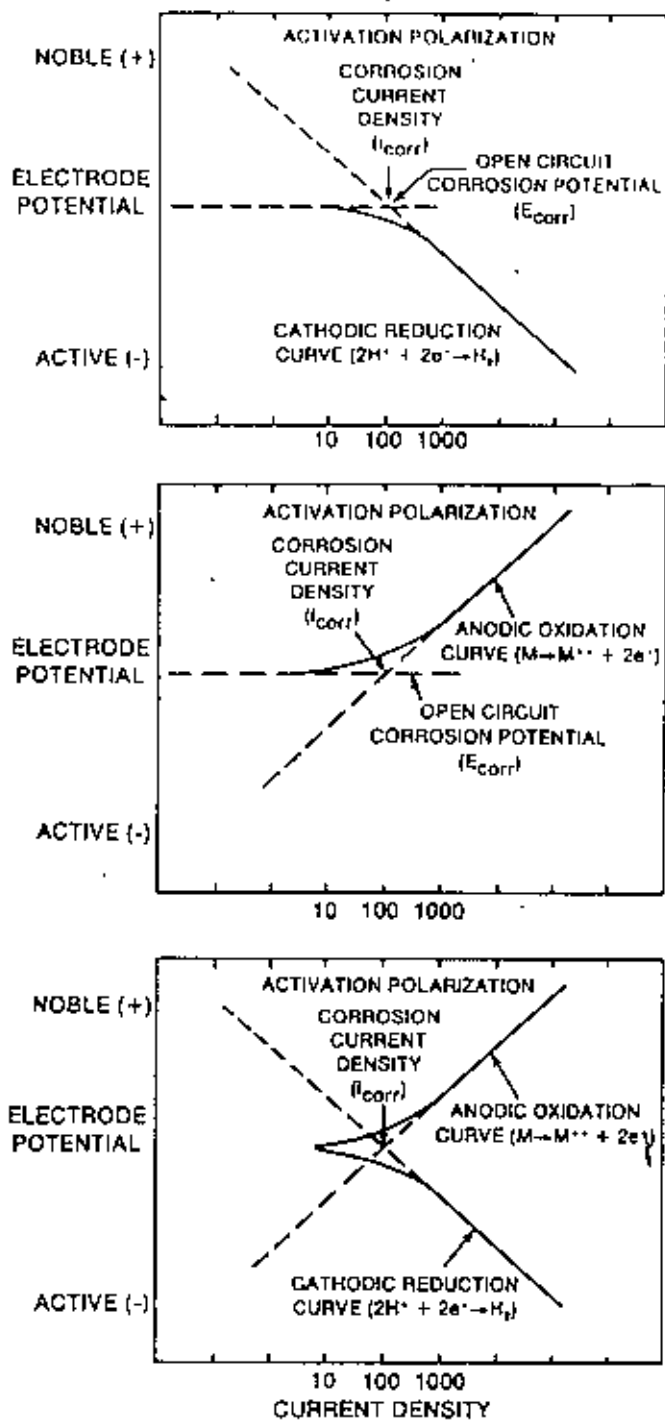


Fig. 2.7 Illustration of three Tafel extrapolation methods of estimating corrosion rate.

These techniques are used in laboratory tests to determine the corrosion rate of a metal or alloy in a specific environment¹⁵. However, they suffer from a variety of drawbacks that limit their usefulness. The resistivity of the solution can contribute significant errors to the estimation of Tafel slopes. The Luggin probe is intended to minimize the solution resistance error. The ideal Luggin probe is a fine capillary that is placed not closer than its outer diameter to the specimen. Closer placement causes errors because the probe shields the specimen. However in dilute solution or when high current densities are employed, the solution resistance errors will be significant. In general, the effect of solution resistivity will be to introduce curvature in the Tafel line so that it is difficult or impossible to obtain an accurate linear portion of the curve that can be extrapolated. One approach has been to draw tangent lines to the measured curves at 50 mV away from the corrosion potential and consider these lines as the Tafel lines.

The effect of solution resistivity on the measured potential may be calculated from Ohm's Law:

$$\Delta E = \rho il \quad (2.12)$$

Where ΔE is the change in measured potential in V, ρ is the solution resistivity in ohm-cm, i is the current density in A/cm², and l is the distance from the specimen to the Luggin tip in cm.

This equation assumes that the potential gradient is linear with distance. The sign of ΔE will correspond to the Stockholm sign invariant convention for potential when the sign of i is based on positive for anodic currents and negative for cathodic currents as per ASTM Standard Practice G3.¹⁴ Equation (2.12) will overestimate resistivity polarization errors in most laboratory cells because the auxiliary electrode area is usually substantially larger than the specimen electrode. However, this equation provides a useful approach for determining when resistivity errors will be significant.

Modern potentiostats often include resistance compensation based on an assumed solution resistance. This approach can help minimize resistance errors if the solution resistance is known and the current employed is relatively low. When high currents are used or tests are conducted in a highly resistive electrolyte such as relatively pure water, a better approach is to use a current interrupter. This is an electronic device that switches off the current briefly while the potential is being measured. The electrode potential decays relatively slowly while the solution resistivity contribution disappears instantly, thus allowing the specimen potential to be measured accurately.

Another source of error in using polarization curves to estimate corrosion rates is the scan rate effect. In order to obtain a true polarization curve, it is necessary to hold the potential constant until a stable current is achieved. In practice, it is normal to use a potentiodynamic scan, which gradually increases the potential and records the current continuously. When coupled with a logarithmic converter and an XY recorder, it is possible to obtain Tafel plots

without the need for calculations or replotting of data. Scan rate effects may cause significant errors in Tafel curve determination when using a potentiodynamic technique. The magnitude of this effect can be estimated by rerunning the curve at a lower potential scan rate and comparing the current values obtained with the currents obtained at the higher rate. If the low scan rate curve shows substantially lower currents at comparable potentials, then it is likely that the scan rate errors are present in the system.

The use of polarization curves to determine corrosion rates has more errors than other techniques available such as the polarization resistance approach. The method is useful because it does provide information on the electrochemical behavior of the system, but it is not unusual to encounter errors of a factor of 2 to 5 when comparing mass loss rates to corrosion current estimates from Tafel extrapolations¹⁶.

2.4.9.2 Polarization Resistance

Another approach to the problem of electrochemical corrosion rate measurement is to apply only a small potential difference to the specimen and measure the current this type of change produces. The potential current density plot is approximately linear in the region within 10 mV of the corrosion potential. The slope of this plot in terms of potential divided by current density has the units of resistance-area and is often called the polarization resistance. This polarization resistance is related to the corrosion current density by the relationship:

$$i_{\text{corr}} = B \frac{i_{\text{net}}}{\Delta E} = \frac{B}{R_p} \quad (2.13)$$

Where $\frac{i_{\text{net}}}{\Delta E}$

is the change in specimen current density per unit change in potential. R_p is the polarization resistance. B is the Stern-Geary constant of the system, and i_{corr} is the corrosion current density.

The Stern-Geary constant is related to the Tafel constants by the relationship:

$$B = \frac{b_a b_c}{2.303(b_a + b_c)} \quad (2.14)$$

Where b_a and b_c are anodic and cathodic Tafel constants respectively, measured on a decade scale.

The value $\frac{1}{R_p}$

is sometimes referred to as polarization admittance.

In order to use this technique, it is, of course, necessary to know the Tafel slopes independently. However, in many cases, reasonable estimates can be made as to what these Tafel slopes should be, and in other cases, the method can be calibrated using mass loss data.

There are two different commercial systems in use for this purpose¹⁵ and they are illustrated in Fig. 2.8. One system employs three electrodes, usually of the same alloy¹⁷. One specimen is the working electrode, while the second electrode is the auxiliary electrode and the third is the reference electrode. The potential

between the working and reference electrodes is monitored; in order to measure the corrosion rate, sufficient current is passed from or to the auxiliary electrode to displace the specimen potential either plus or minus 10 mV. The current flowing is then proportional to the corrosion rate. The size of the electrode is adjusted so that the same instrumentation can be used for each alloy. Instrumentation is available that can measure the current with either positive, negative, or alternating polarization.

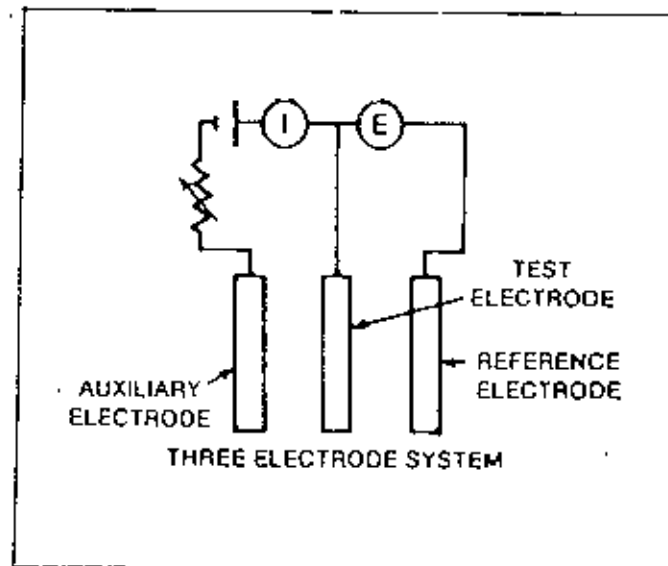


Fig. 2.8 Polarization resistance probes.

2.4.9.3 Small Amplitude Polarization Techniques

The polarization resistance technique uses a single finite polarization potential, usually 10 mV, to estimate the polarization resistance. If a potentiodynamic approach to polarizing the specimen is available, then more sophisticated analyses can be performed. The simplest approach is to use a constant scan rate polarization and obtain a plot of current versus potential. If the scan direction is reversed at some point, e.g. 10 mV, then a hysteresis curve will be generated. This approach is sometimes referred to as small amplitude cyclic voltametry (SACV). If the hysteresis is significant, then the potential scan rate is probably too high and the run should be rerun at lower rate until hysteresis is no longer observed.¹⁸ The slope of the potential-current curve at zero polarization is then the polarization resistance.¹⁹

2.4.9.4 General Polarization Techniques

Polarization techniques have been used for years to characterize the corrosion behavior of metal alloys in specific environments. The approach is to immerse the specimen in an environment that does not have oxidizing agents present, such as oxygen, ferric ions, chromate's, etc. The metal specimen is then polarized anodically to determine its corrosion current as a function of oxidation potential. This approach is particularly desirable for metals showing passivity, such as stainless steel and related alloys. A typical polarization curve for AISI 430 SS is shown in Figure 2.9. The anodic current at potentials greater than 50 mV more noble than the open circuit potential should approximate the actual

corrosion current at these potentials. However, it must be realized that the current values obtained are very dependent on both the solution conditions and the polarization method. This technique can be used to evaluate different alloys over a range of oxidizing conditions if the other conditions are held constant.

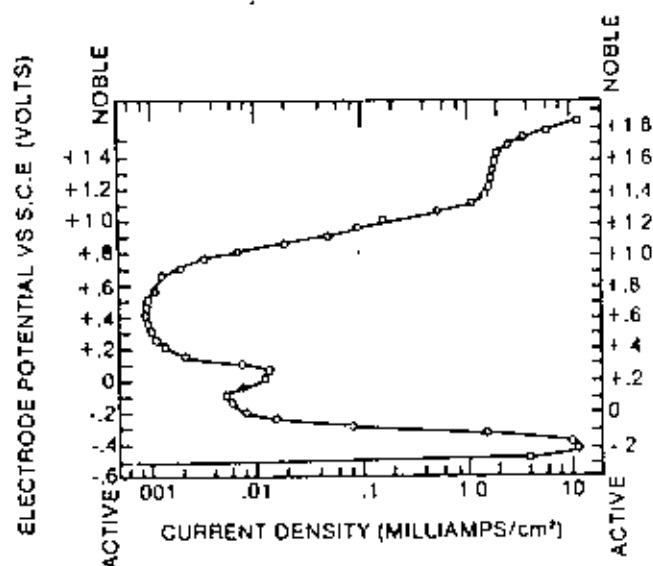


Fig. 2.9 Polarization curve for AISI 430 SS in 1.0N sulfuric acid at 30°C.

Modern instrumentation has greatly simplified the procedures required to obtain useful results. The potentiostat, electrometer, logarithmic converter, potential programmer, recorder and data acquisition system can be obtained as single console. Similarly, the electrochemical cells used to conduct corrosion tests have been developed to allow both cylindrical and flat specimen configurations. The traditional polarization cell²⁰ is shown in Figure 2.10. In carrying out polarization diagram measurements, it is important to deaerate the system thoroughly and to guard against crevice

corrosion. This is especially important in systems that show active-passive behavior.

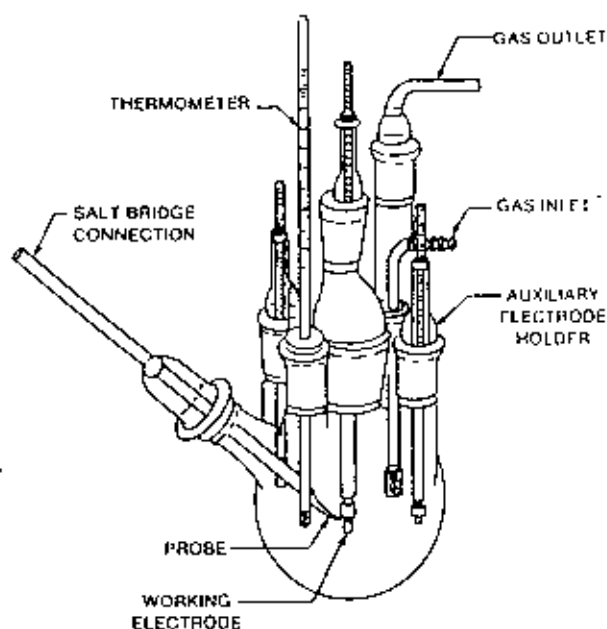


Fig. 2.10 Standard multineck polarization cell.

The electrolyte corrosion (EC) test²¹ is an example of a polarization technique that is used to simulate extended atmospheric service on plated parts. This test was developed as a rapid evaluation technique for automotive parts with decorative multiple layer copper (optional)-nickel chromium plating systems. The specimen is masked to exclude insignificant areas from the test, and the test area is scrubbed with a MgO slurry to clean it. The specimen is then immersed in an acidic sodium nitrate, sodium chloride solution and polarized for a series of 1 min intervals. The polarization potential is + 0.300 V relative to a saturated calomel electrode. After each interval, the corrosion is evaluated by means

of an indicator solution that reveals penetration by the corrosion process to the base metal. Each period of two minutes is approximately equivalent to one year automotive service exposure in Detroit, Michigan. A commercial test instrument is available.

The EC test has been standardized by ASTM Committee B8 as Standard Method B627 for evaluation the corrosion resistance of copper-nickel-chromium electrodeposits on steel and zinc base die castings designed for outdoor service²² The results of the test are reported as the number of corrosion sites that develop at the end of each exposure cycle.

CHAPTER: THREE

3. Experimental

3.1. Electrodeposition

3.1.1 Preparation of the Substrate for Electrodeposition

Locally manufactured mild steel sheet of size 5cm x 2.5cm x 0.13cm was used as the substrate and the anode was a platinum sheet of similar dimension.

The flow diagram of substrate preparation is as follows:

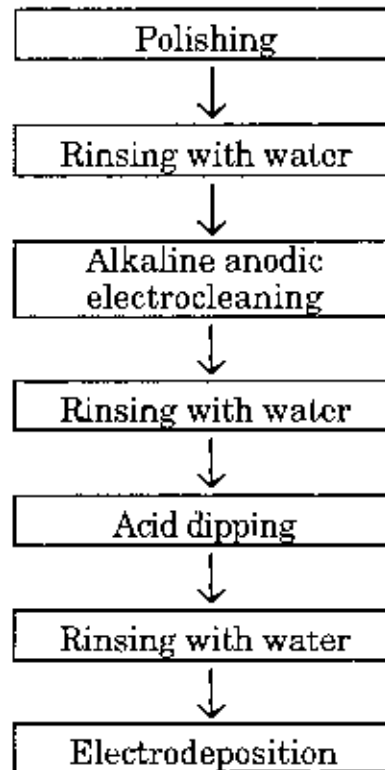


Fig. 3.1 Flow chart of pretreatment operations applied to substrate before electrodeposition.

Polishing: The cathode was mechanically polished with progressively finer grades of emery paper, first with grade no. 3 then with 2 and 1 and finally with no. 0.

Rinsing: Thorough rinsing was done to obtain a clean, stain free and dust free surface necessary for subsequent electrocleaning operation. In order to get optimum rinsing conditions, maintenance of the high pressure cold water sprays were provided.

Anodic electrocleaning: The substrate was cleaned electrochemically in a strongly basic solution. [Composition and operating condition described in Table 3.1]. This treatment removes greases, metallic oxides and smuts from the substrate surface.

Acid dipping: Electrocleaned samples were acid dipped to neutralize and remove any residual alkali film, oxides and smuts and to activate the work piece for subsequent electroplating. Various parameters of the treatment are given in Table 3.1. After the acid dipping the substrate was rinsed in distilled water kept at room temperature. The substrate is now ready for electrodeposition.

Table 3.1 Particulars of electrocleaning and acid dipping operations

Name of Operation	Reagents used		Operating Condition		
	Formula	Concentration g/l	Temp °C	Current density mA/cm ²	Time s.
Anodic electrocleaning	Na ₂ CO ₃	35	45 ⁰	60	60
	NaOH	25			
Acid dipping	HCl	30	Room	-	30

3.1.2 Electrodeposition Set-Up

The experimental set-up for the electrodeposition process consisted of a 500 c.c. beaker, a D.C. power supply, a thermometer, a magnetic stirrer, a stand and perspex holder.

The beaker containing 400 c.c. electrolyte and magnetic stirrer was placed on a magnetic hot plate so as to be able to agitate the electrolyte. Anode and cathode were connected to a D.C. power supply via a milliammeter. Two anodes were placed on both sides of the cathode for uniform deposition on both sides of the cathode. Schematic of the set-up used for electrodeposition is shown in Fig. 3.2.

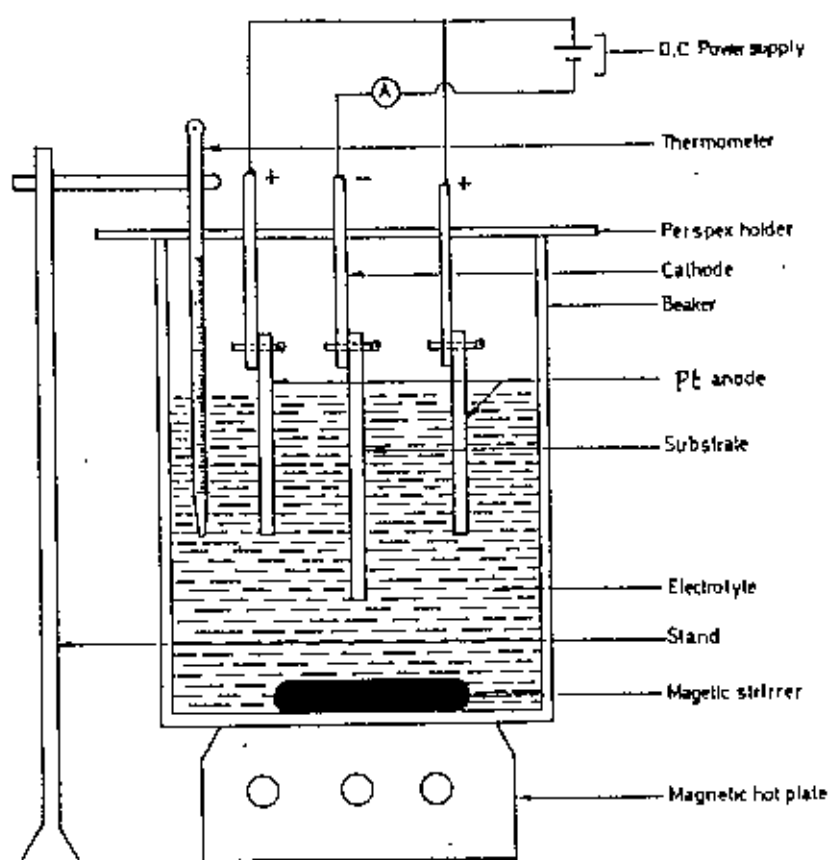


Fig 3.2 Electrodeposition set-up.

3.1.3 Electroplating Operation

Electrodeposition of Zn-Ni alloy was made on mild steel substrate using the set-up shown in Fig. 3.2.

Deposition was carried out galvanostatically at current densities of 40, 60 and 80 mA/cm². Sulphate based plating baths of various formulations with pH in the range of 2-4 were utilized for the deposition experiments (Table 3.2). The solutions were prepared using distilled water and reagent grade chemicals. pH was adjusted by adding sodium hydroxide solution. Zn-Ni alloy electrodeposits were made at 45°C. Some electrodeposits were also prepared at 25°C. After deposition, coated substrate was washed with distilled water, dried in hot air and stored in a desiccator for further investigation.

Table 3.2 Plating baths and parameters used in this study.

Bath constituents	Concentrations g/l			
	Bath-I	Bath-II	Bath-III	Bath-IV
NiSO ₄ .6H ₂ O	150	285	280	-
ZnSO ₄ .7H ₂ O	290	150	285	240
H ₃ BO ₃	30	30	30	-
NH ₄ Cl	-	-	-	15
Deposition Temperature	25°C & 45°C	25°C & 45°C	25°C & 45°C	25°C & 45°C
pH	2-4	2-4	2-4	2-4

3.2 Chemical Analysis of Coatings

The Zn-Ni alloy coating was chemically analysed for nickel content mainly by atomic absorption spectroscopy (AAS). Conventional wet chemical analysis was also performed in some cases for comparison purposes.

3.2.1 Chemical Analysis of Coating by Atomic Absorption Spectroscopy (AAS)

For chemical analysis the coatings were deposited on passivated stainless steel substrate which allows easy separation of the coatings. The stainless steel substrate were passivated before electrodeposition by rubbing it with MgO and then dipped in concentrated $K_2Cr_2O_7$ solution for 5 minutes. Stainless steel thus passivated were cleaned in distilled water and used for Zn-Ni alloy deposition. After deposition, the coatings were peeled off, and 10 mgs of the same were dissolved in 1:1, HCl. The solution was then diluted to about 5 ppm nickel for AAS measurement.

Standard solutions containing 0.5, 1.0, 2.0, 3.0, 4.0 ppm nickel were made using nickel sulphate salt. These solutions were employed to draw the working curve for AAS. The curve with which the composition were determined is shown in Fig. 3.3. A Simadzu AA-680/G, V-3 atomic absorption spectrometer was used in this study.

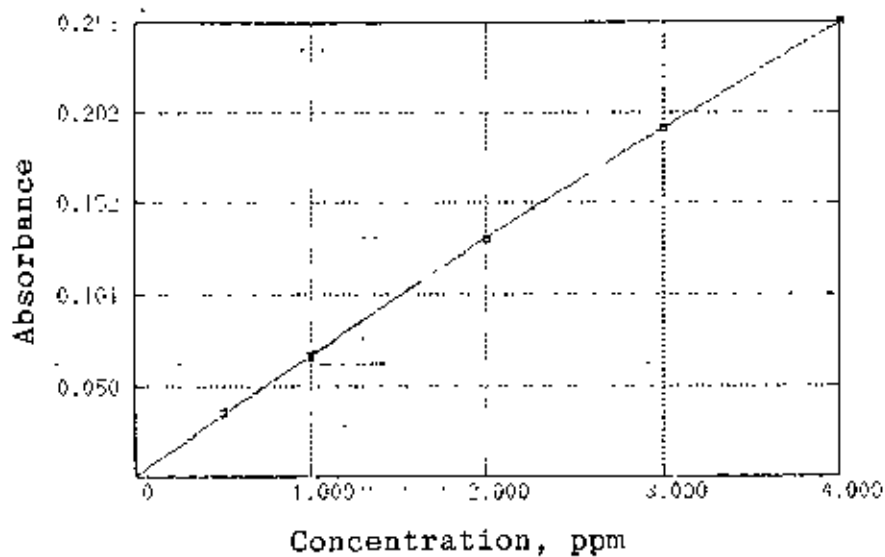


Fig. 3.3 Working curve for composition measurement by AAS.

3.2.2 Analysis of Coating by Conventional Wet Chemical Method

In some cases, the composition of Zn-Ni alloy coatings were determined by chemical analysis by using the dimethyl glyoxime method. The weighed amount of coating was first dissolved in 1:1 HCl and heated. At neutral point dimethyl glyoxime [$C_4H_8N_2O_2$] was added. Ni-glyoxime precipitate of blood red colour was formed which was separated by filtering through a dual filter paper of equal weight. The filtrate was treated several times with NH_4OH , dimethyl glyoxime in sequence until precipitation was completed. The precipitate was then washed several times with hot water, dried in an oven at $110-120^{\circ}C$ for 1 hr, and weighed as $NiC_8H_{14}O_4N_4$ which contain 20.32% nickel.

3.3 Determination of the Coating Thickness

The coated samples were cut into two pieces with a hacksaw blade. The cross sectional sample was mounted and polished with standard grades emery papers of increasing fineness. Final polishing was done in a velvet cloth soaked with a slurry of 1 μ m gamma alumina powder. The thickness of the coating was determined under an optical microscope fitted with a micrometer eye piece. These measurements were used to determine the time to deposit a constant thickness (30 μ m) of Zn and Zn-Ni coating used for various corrosion tests.

3.4 X-Ray Diffraction Studies

Phase structure of both as-deposited and heat treated coatings were investigated by means of X-ray diffraction. X-ray diffraction study was done in a JEOL- JAPAN, Model - JDX - 8P diffractometer using $\text{CuK}\alpha$ radiation at 30kV and 15 mA. The patterns were recorded in a chart recorder. Scan rate and full scale intensity of 2 $^\circ$ / min and 8 x 10³ c.p.s. respectively were used. The operating conditions of X-ray diffractometer are summarized in Table 3.3

Table 3.3 Operating conditions of X-ray diffraction

Radiation	:	CuK α
Voltage and Current	:	30 kV, 15 mA
Scanning Speed	:	2 $^{\circ}$ / min
Chart Speed	:	10 mm / min
Range	:	30 $^{\circ}$ - 90 $^{\circ}$

3.5 Corrosion Test

The following corrosion tests on both pure zinc and zinc-nickel alloy coatings on steel substrate were done to compare their corrosion resistance. For all corrosion tests Zn-6%Ni alloy coating was used.

3.5.1 Salt Water Immersion Test

The Zn-6%Ni alloy and pure zinc coated steel strip was masked with plastic adhesive tape exposing a coated area of 3 cm x 2 cm. Each of the samples was dipped in 3% NaCl solution at room temperature in a conical flask as shown in Fig. 3.4. Dipping was accomplished by hanging the samples with a nylon wire tied to a small hole drilled on the sample. The progress of corrosion of the sample was followed by visual examination and the time taken to form both white rust and red rust was noted. A parallel salt water immersion test was conducted to follow rate of corrosion based on weight loss measurement as a function of immersion time. For this purpose, the sample was taken out of the salt solution after a predetermined time period. This was washed thoroughly in running

water with the help of a plastic brush to remove the corrosion products. The sample was then dried in ethanol and weighed in a digital balance having an accuracy of ± 0.1 mg. The weight of the sample thus obtained was subtracted from the initial weight to find the weight loss due to corrosion. The corrosion rate was then calculated in terms of mils per year (mpy) following the procedure described in @ 2.4.6.

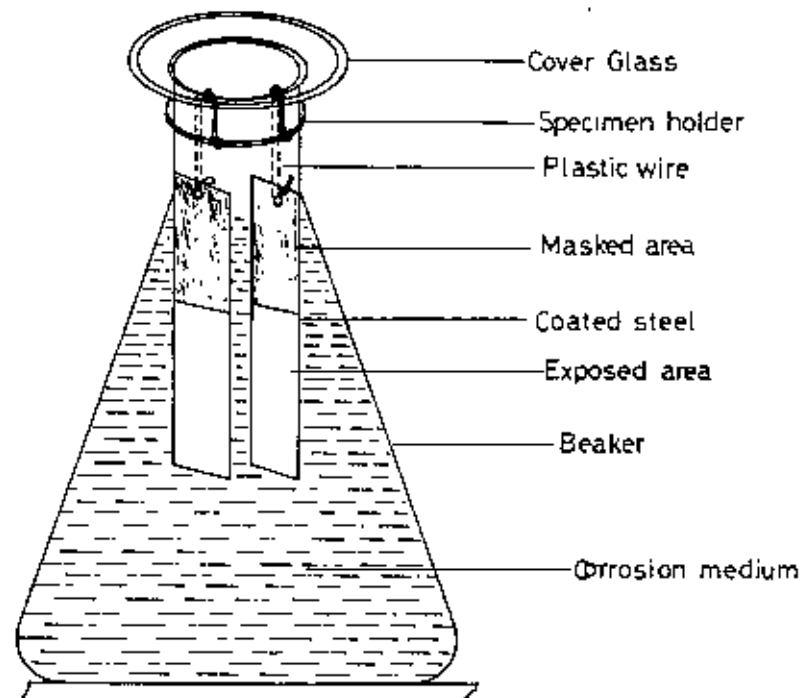


Fig. 3.4 Dipping test set-up

3.5.2 Hot Water Immersion Test.

The coated samples were immersed in hot water at $80 \pm 2^\circ\text{C}$ for 4 hours. The set-up consists of a conical flask put on a hot plate. The samples were hung using the same procedure as described in section 3.4.1. At the end of the experiment, the sample was taken out, washed with a brush in running water, dried with ethanol and weighed. The sample was examined visually and the weight loss due to corrosion was calculated.

3.5.3 Electrochemical Corrosion Test

Electrochemical corrosion tests were done by using a potentiostat (Model: HA-303) in a conventional three electrode cell. A platinum sheet was used as counterelectrode and a saturated calomel electrode (SCE) used as the reference electrode. Both anodic and cathodic polarization behavior were recorded. During the tests, applied potential was incremented by 50 mV and the corresponding current density measured. Current density at each applied potential was recorded about three minutes after the application of the potential, during which period the cell current reached a steady state value. From these data, polarization curve were drawn for both pure zinc coating and Zn-6%Ni alloy coatings.

The electrochemical corrosion tests were performed in NaCl solutions of various compositions. Additional experiments were conducted using solutions containing various amount of Na_2S and FeCl_3 as these may be present as contaminants in different corrosion environments. The solution compositions are given in

Table 3.4. During the polarization tests, a fixed area of the coating (3cm x 2cm) was exposed to the solution. All polarization measurements were carried out at room temperature.

Table 3.4 Corrosion medium used for electrochemical corrosion test.

Solution	Composition, %		
Designation	NaCl	Na ₂ S	FeCl ₃
1	1.5	-	-
2	3.0	-	-
3	4.5	-	-
4	3.0	0.1	-
5	3.0	0.2	-
6	3.0	-	0.1
7	3.0	-	0.5
8	3.0	-	1.0

CHAPTER: FOUR

4. Results and Discussion

4.1 Electrodeposition of Zinc-Nickel Alloy

4.1.1 Effect of Deposition Current Density

The effect of deposition current density on the composition of the deposit obtained from different plating baths is shown in Fig. 4.1. It is seen from the figure that the nickel percentage in the deposit remains almost constant with current density in bath I and III. In the case of bath II however, nickel content is seen to increase when current density increases above 60 mA/cm^2 . It is further seen that nickel percentage is the highest in deposits obtained from bath II. Deposits from bath I have the lowest nickel content while those from bath III have an intermediate nickel content. It may be recalled in this connection that the nickel contents of bath I, II and III are 32%, 63% and 47% respectively. It is thus expected that bath having highest nickel content would result in deposits with the highest percentage of nickel.

Conflicting information is available in the literature on the relationship between nickel content of deposits and current density. Schoch and Hirsch¹¹ reported that the nickel content of zinc-nickel alloy deposits remains almost constant up to a current density of about 25 mA/cm^2 above which a slight increase in nickel content is observed. On the other hand, Escher et al.¹² observed that in the

lower current density range (up to 30-40 mA/cm²), nickel content of the deposit decreases with current density. At higher current densities (40-70 mA/cm²), nickel content of the deposit becomes almost independent of the current density. Recently, Albalat et al.³ reported that the nickel content of zinc-nickel alloy deposit is independent of current density in the range of 15-60 mA/cm².

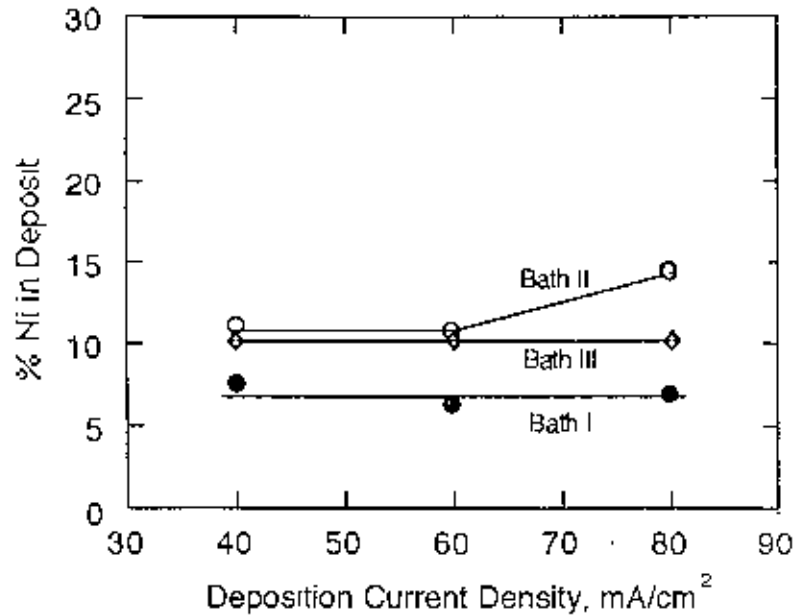


Fig. 4.1 Effect of current density on the percentage of nickel in electrodeposited Zn-Ni alloys.

In the present study, nickel content of the deposits is independent of current density for baths I and III. However, for bath II which contains the highest percentage of nickel, an increase in nickel percentage in the deposits is observed at current density above 60 mA/cm². This behavior resemble the finding of Schoch and Hirsch¹¹. This increase in nickel content at higher current density could be linked to the fact that zinc is the readily depositable metal

and hence is under diffusion control during zinc-nickel alloy deposition⁶. An increase of current density is therefore borne mainly by the less readily depositable nickel. This increase particularly happens in bath II because of its high nickel content.

4.1.2 Effect of Bath Composition

The influence of nickel percentage in the bath on the electroplated alloy composition is shown in Fig. 4.2. A composition reference line is also shown in the figure. Points falling upon the composition reference line would represent alloy having the same percentage composition as the metal percentage of the bath. A composition curve that rises above the composition reference line indicates that the metal in question is preferentially deposited, because its percentage in the deposit is larger than its metal percentage in the bath. In normal codeposition, the more noble metal deposits preferentially, hence the curve for the percentage of more noble metal in the deposit always lies above the composition reference line. Similarly, the curve representing the percentage of the less noble metal plotted against its metal percentage in the bath lies below the composition reference line.

It is seen in Fig. 4.2 that the curve relating the nickel percentage in alloy with nickel percentage of bath lies below the composition reference line. This means that nickel, in spite of being the more noble metal, deposits less readily. This further implies that the less noble metal zinc deposits preferentially under the deposition conditions used. Such anomalous type of codeposition in the zinc-nickel system has earlier been reported by others.^{2, 23}

9/1/2020

Albalat et al.³ working on the chloride based bath also reported similar observation. It is further observed in Fig. 4.2 (thick line) that the percentage of nickel in the deposit increases linearly with the nickel percentage in the bath. This reconfirm the observation of Moniruzzaman²³. Such linear dependency was also noticed for chloride based baths^{3, 10}.

Several theories have been proposed to explain the anomalous codeposition in the zinc-nickel system. Knodler²⁴ and Fukushima et al²⁵ suggested that a local increase in pH during deposition induces zinc hydroxide precipitation which inhibits the nickel discharge. Swathirajan²⁶, proposed that underpotential deposition of zinc on nickel nuclei plays a role on the anomalous codeposition of zinc-nickel alloys.

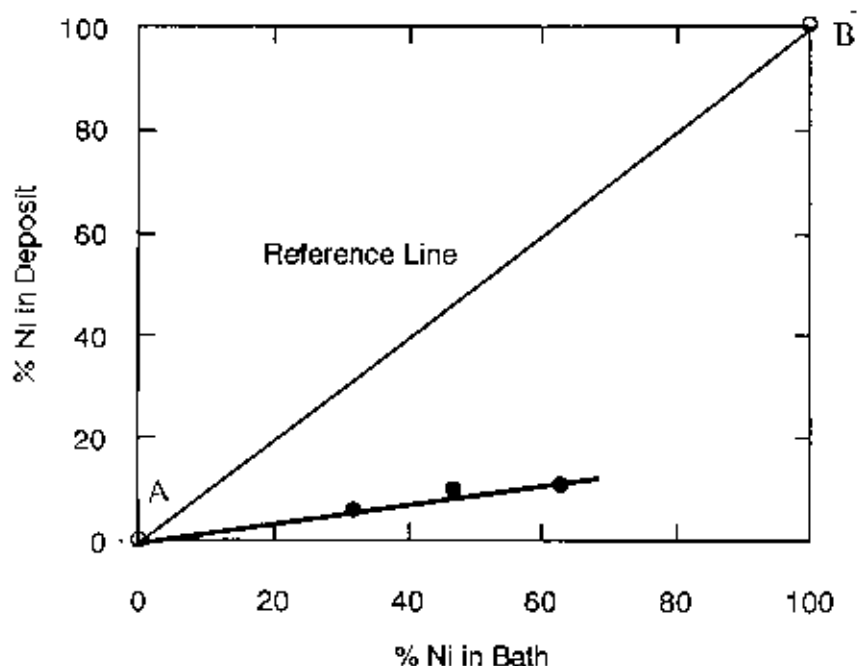


Fig. 4.2 Relation between the composition of the deposit and the composition of the bath in Zn-Ni alloy deposition.

4.1.3 Effect of Bath Temperature

The effect of temperature on the alloy composition was investigated taking the bath and other operating conditions fixed. The results are listed in Table 4.1. The effect of increasing temperature at a given current density is to increase the nickel content in the deposits.

Table 4.1 Effect of temperature on the alloy composition (Bath III)

Deposition current density mA/cm ²	Temperature °C	%Ni in Deposit
40	25	2.8
	45	10.18
60	25	4.1
	45	10.21
80	25	4.3
	45	10.22

Mathias et al.¹⁰ found that at current densities less than 300 mA/cm² the effect of increasing the temperature at a given current density is to increase the nickel content of the deposit. However, at higher electrolyte velocity, increasing the temperature may result in a decrease in nickel content. This is because at higher velocity, deposition of zinc becomes mass transfer controlled¹⁰ Since temperature improves mass transfer, increasing deposition temperature will result in a higher zinc content at very high electrolyte velocity.

In the present case where very mild agitation was used during deposition, an increase in bath temperature is therefore expected to increase the nickel content of the deposit.

4.1.4 Effect of pH

During the electroplating experiments it has been observed that the pH of the plating bath has a great influence on the quality of the zinc-nickel alloy deposits. In the pH range of 2-4, uniform and adherent coatings were obtained. At pH > 4 coatings become non-adherent and brittle. While at pH < 2 deposit was seen only near the edge of the substrate and the middle portion of the substrate remained bare.

According to the Pourbaix diagram of nickel²⁷ precipitation of Ni(OH)₂ can take place at pH greater than 5.8. Due to the discharge of hydrogen at the cathode, hydrogen ion concentration at the cathode diffusion layer is lowered which consequently increases the pH locally²⁸. Under this condition, pH at the cathode diffusion layer could reach values higher than 5.8, although the bulk pH may remain slightly above 4. As a result Ni(OH)₂ can precipitate in the diffusion layer. Inclusion of the basic hydroxide into the deposit is believed to cause brittleness in zinc-nickel alloys obtained from bath with pH > 4. It is believed that at pH < 2, zinc-nickel plating baths becomes rather corrosive and hence attacks the deposited alloy chemically. At the middle portion of substrate where current density is lower than the average, the rate of chemical attack is higher than the deposition rate. On the other hand, the rate of deposition is higher than the rate of chemical attack near the edges

of the substrate where the current density is higher than the average. Consequently significant amount of zinc-nickel alloy deposit could only be seen at the edges at pH lower than 2.

In the present study pH of the deposition bath was maintained at 2-4 by the addition of sodium hydroxide from time to time.

4.1.5 Phase Structure of Coatings

X-ray diffraction patterns of pure zinc and Zn-6%Ni alloy coatings in the as-deposited condition are shown in Fig. 4.3. and 4.4 respectively.

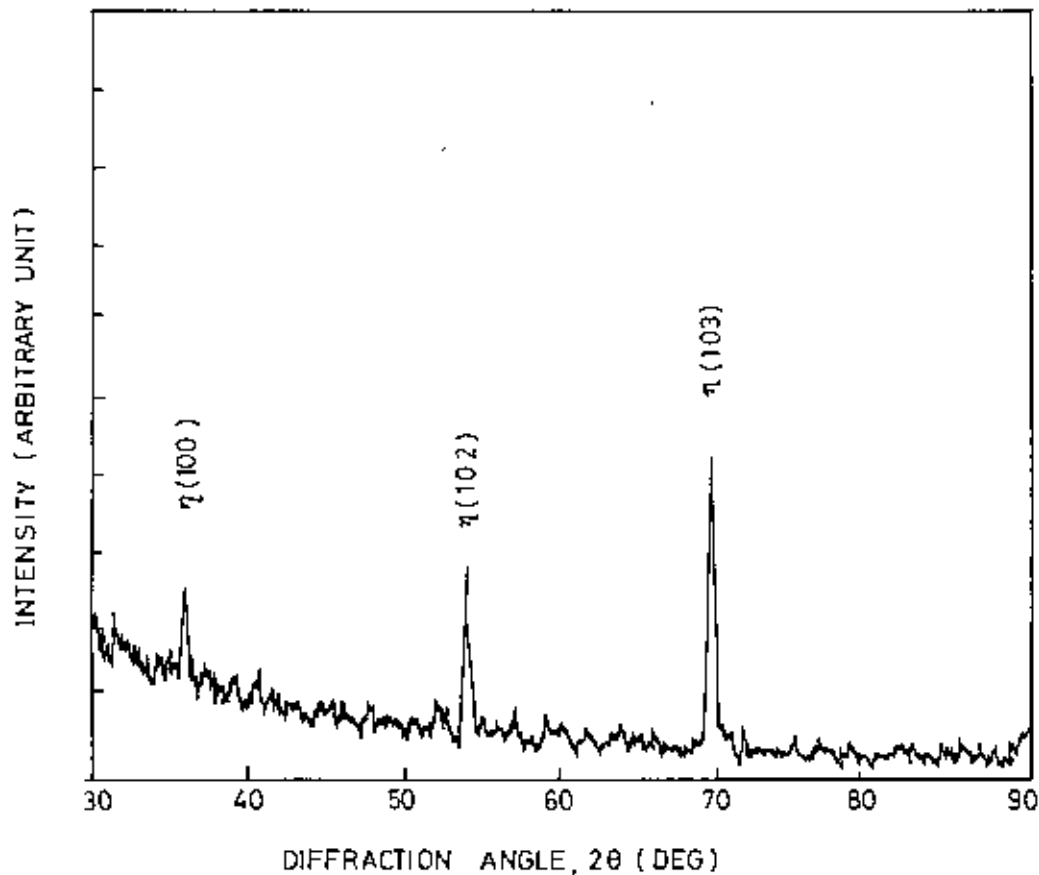


Fig. 4.3 X-ray diffraction pattern of pure zinc coating in the as-deposited condition

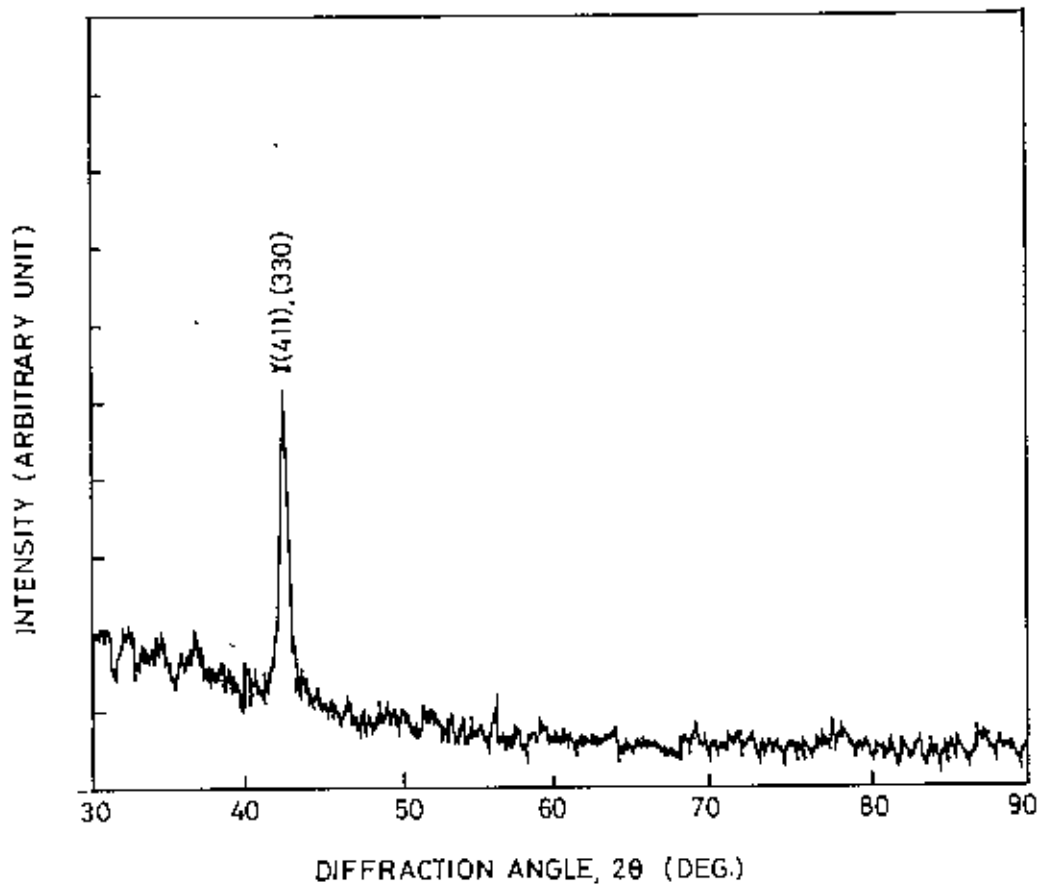


Fig. 4.4 X-ray diffraction pattern of Zn-6%Ni alloy coating in the as-deposited condition.

In the as-deposited condition zinc and zinc-nickel alloy coatings seen to exhibit diffraction peaks of η and γ phases respectively. Both coatings are found to be in a textured state. Zinc coating has a (103) texture, while Zn-6%Ni coating possesses a $\gamma(411), (330)$ texture.

The diffraction pattern of Zn-6%Ni alloy coatings in the annealed condition is shown in Fig. 4.5.

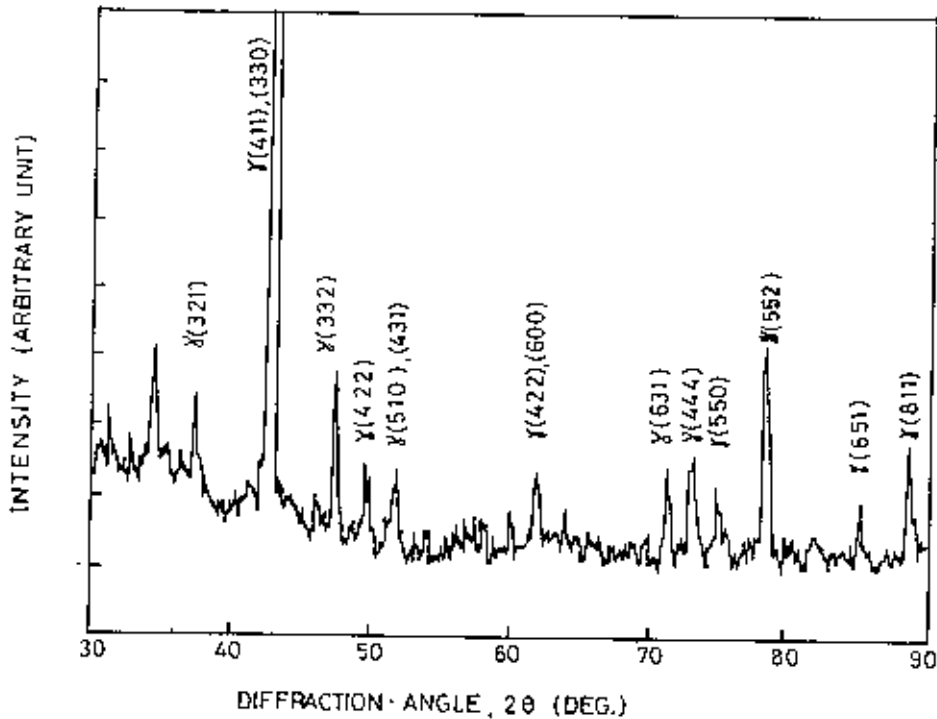


Fig. 4.5 X-ray diffraction pattern of Zn-6%Ni alloy coating in the annealed condition (Annealing temperature and time: 300°C and 60 minutes).

A comparison of Fig. 4.4 and Fig. 4.5 shows that a number of additional peaks appeared in the pattern of the zinc-nickel alloy after annealing. These peaks are indexed to be mostly of the γ -phase. Moreover, the sharpness and intensity of $\gamma(411)$, (330) peak is found to be have increased upon annealing. These indicate that the as-deposited coating of zinc-nickel alloy is in a stressed and / or fine grained state. Annealing is thought to remove the internal stress as well as increase the grain size leading to the sharpening of the peaks. Furthermore, annealing is found to cause the removal of texture of zinc-nickel alloy coating.

4.2 Corrosion Behaviour of Zinc and Zinc-Nickel Alloy Coatings

For zinc-nickel alloy sample preparation used in corrosion studies, bath I and cathodic current density of 60 mA/cm^2 were chosen. Under these conditions, very uniform and adherent coatings of zinc-nickel alloy with 6% nickel were obtained. A deposition time of 30 minutes was used to deposit Zn-6%Ni alloy coatings with a thickness of $30\mu\text{m}$. This required deposition time was found out through microscopic study from a number of trial experiments.

For comparative corrosion studies, $30\mu\text{m}$ thick pure zinc coating was deposited from bath IV using a current density of 60 mA/cm^2 for 25 minutes. In order to investigate the corrosion behaviour of the coating comprehensively, a number of corrosion test methods viz; hot water immersion tests, salt water immersion tests and electrochemical corrosion tests were employed. The results obtained in these experiments are described and discussed in the sections to follow.

4.2.1 Corrosion in Hot Water

The results of hot water immersion test are summarized in Table 4.2. It is seen in Table 4.2 that no red rust was formed on both zinc and Zn-6%Ni alloy coatings. The hot water corrosion test as described earlier @ 3.4.2 is a short time corrosion test. This test discloses discontinuities or porosity in coatings which would result in rapid failure of coatings. It also determines the degree of protection of zinc coatings against formation of white corrosion products. In the absence of any spots of red rust, it is concluded that the coatings of zinc and zinc-nickel alloy used in the present study are rather uniform, defect free and continuous. There are no discontinuities in both the coating through which the substrate could be attacked in this short experimental duration resulting in the formation of red rust. The appearance of Zn-coating however changed into dark colour while the Zn-Ni alloy coating remained almost the same as before. No weight loss could be detected for both coatings during the hot water immersion test.

Table 4.2 Corrosion behavior of various coatings in hot water immersion test.

Coating type	Temperature of water (°C)	Exposure time (h)	No. of red rust formed
Zn-Coating	80±2	4	nil
Zn-Ni alloy coating	80±2	4	nil

4.2.2 Salt Water Corrosion

Zinc as well as zinc-nickel alloy coated steel samples were immersed in aqueous solution of 3% NaCl. The extent of corrosion damage was evaluated qualitatively by visual inspection. Parallel sets of experiments were also conducted in the same solution and corrosion resistance of the coatings were evaluated quantitatively on the basis of weight loss measurements.

When zinc and zinc-nickel alloy coatings are exposed to salt solutions, hydroxide of zinc forms as corrosion product. This product is known as white rust because of its colour. Upon further exposure, the coatings get damaged at places and the substrate is exposed. Formation of the characteristic red rust (hydrated oxides of iron) then takes place on the exposed steel surface and it eventually covers the whole specimen. It was found that on zinc coating, the surface was covered completely by white rust after about 7 days. But on Zn-6%Ni alloy coating, white rust did not cover the surface completely. Coverage by white rust reaches a steady state value of about 25% after about 60 days. Table 4.3 shows the time required for the formation of red rust on zinc and zinc-nickel alloy coated steel as well as on the bare mild steel substrate. Formation of red rust on mild steel occurred only two days after immersion. Zinc coating on mild steel deferred red rust formation for about 55 days. On the other hand, it took 120 days for the formation of red rust on mild steel coated with Zn-6%Ni alloy.

Table 4.3 Corrosion behaviour of coatings and substrate in 3wt%NaCl solution.

Coating type	Coating thickness (μm)	Time to form red rust (day)
Zn-Coating	30	55
Zn-6%Ni alloy coating	30	120
Bare steel substrate	-	2

Pushpavanam et al.⁵ reported on the comparative corrosion resistance of zinc and zinc-nickel alloys deposited from zinc sulphate-nickel sulphamate baths. They found in salt spray test that the time required for the formation of red rust was about twentyfive percent longer for Zn-5%Ni alloy coating as compared with that for pure zinc coating.

Fig 4.6.a & 4.6.b show the photograph of zinc and Zn-6%Ni alloy coated samples respectively after an immersion, period of two months in 3wt%NaCl solution. Zinc coated sample is seen to be completely covered by red rust.

This indicate that the zinc coatings have corroded and disappeared all together after two months of immersion. Consequently the corrosion of bare steel substrate yielded red rust. On the other hand, the greyish zinc-nickel alloy coating still remain intact. No red rust formation is visible on the sample after two mouths of immersion.

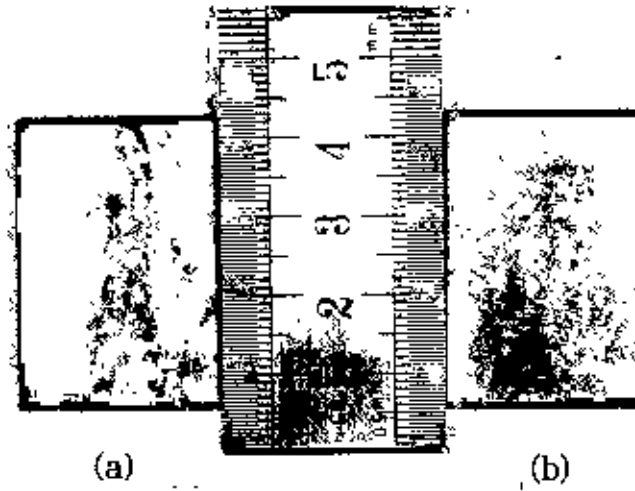


Fig. 4.6 Photograph of (a) zinc and (b) Zn-Ni alloy coated steel after dipping in 3% NaCl solution for 2 months.

Fig. 4.7 shows quantitatively the relative corrosion resistance of zinc and zinc-nickel alloy coatings in terms of corrosion rate expressed in mpy . It is seen that the corrosion rate of both coating increases with immersion time. Corrosion rate of Zn-6%Ni alloy coating is found to be always lower than that of pure zinc coating. The rate of increase of corrosion rate with immersion time is lower for the zinc-nickel alloy coating. After an exposure period of twelve days, corrosion rate of zinc-nickel alloy coating is found to be one-third that of pure zinc coating. Corrosion of zinc coating reaches a steady-state condition after about 10-12 days while Zn-6%Ni alloy does not show any such state. Further study is necessary to find out the reason of such behaviours.

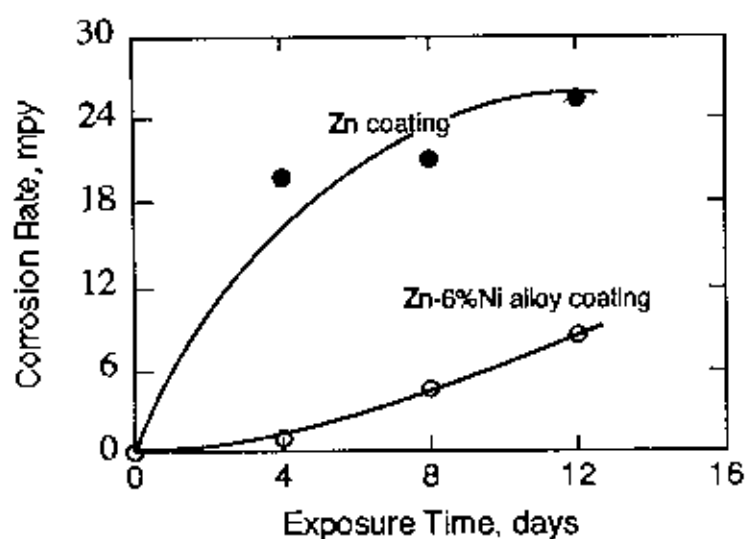


Fig. 4.7 Relative corrosion resistance of Zn and Zn-6%Ni alloy in terms of mpy.

4.2.3 Electrochemical Corrosion

The rest potentials of zinc and Zn-6%Ni alloy coatings in various corrosion medium are given in Table 4.4. The rest potential of mild steel substrate is also given in the table for comparison. It is seen that both zinc and zinc-nickel alloy coatings are less noble than mild steel. Thus both coatings have the ability to provide galvanic protection to steel. Presence of Na_2S or FeCl_3 is seen to shift the rest potential of both samples. Giridhar and van Ooij²⁹ measured the rest potential of zinc and zinc-nickel alloy coatings in 3wt%NaCl. The rest potential values obtained in the present study in 3wt%NaCl solution are similar to those reported by Giridhar and van Ooij.

Table 4.4 Rest potentials of coatings and mild steel substrate in various medium.

Corrosion medium		Rest potential, mV (vs. SCE)		
%NaCl	%Other addition	Zn	Zn-6%Ni	Mild steel
1.5	-	-1030	-945	
3.0	-	-1055	-970	- 340
4.5	-	-1045	-950	
3.0	0.1Na ₂ S	-1040	-1050	
3.0	0.2Na ₂ S	-1090	-1070	
3.0	0.1FeCl ₃	-1100	-1100	
3.0	0.5FeCl ₃	-1060	-1020	
3.0	1.0FeCl ₃	-1020	-990	

The anodic polarization curves for electrodeposited pure zinc and Zn-6%Ni alloy coatings in NaCl solution of various composition are presented in Fig. 4.8.

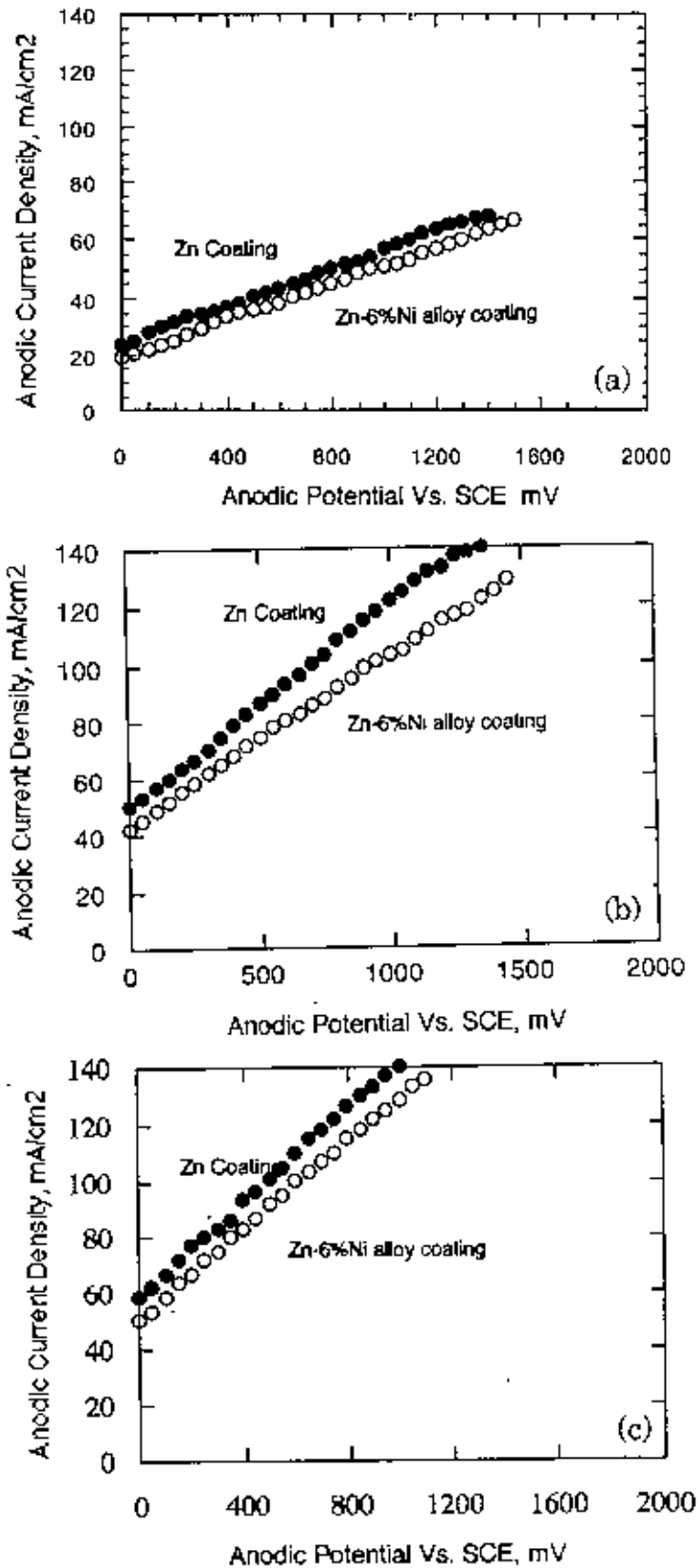


Fig. 4.8 Anodic polarization curves for electrodeposited pure zinc and Zn-6%Ni alloy coatings in (a) 1.5%, (b) 3.0% and (c) 4.5% NaCl solution.

As applied electrode potential is made more positive the coatings dissolution rate increases which is indicated by the increase in anodic current density. From the Fig. 4.8 it is seen that the anodic current density on pure zinc coating is always higher than that on Zn-6%Ni alloy. A comparison of the anodic current density for same applied potential reveal that the rate of corrosion is lower for Zn-6%Ni alloy than that for pure zinc. As the concentration of NaCl solution increases the corrosion rate of both zinc and Zn-6%Ni alloy increases. This is detected by the increase in slope of the anodic current density versus potential curves with the increase of sodium chloride concentration from 1.5 to 4.5%.

Current density at zero applied potential on zinc and the zinc-nickel alloy coatings are given in Table 4.5. It is seen that increasing chloride ion concentration tends to increase the anodic current density at the rest potential. However, this increase becomes less pronounced beyond the NaCl concentration of 3% in the case of both pure zinc and zinc-nickel alloy coatings.

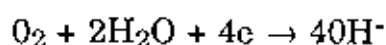
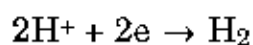
Table-4.5 Anodic current density at zero applied potential in solution containing different amount of sodium chloride.

% NaCl	Anodic current density at zero applied potential, mA/cm ²	
	Zn	Zn-6%Ni
1.5	23.3	18.3
3.0	50.0	41.6
4.5	58.3	50.0

The coating in the NaCl solution are galvanically coupled with platinum during the electrochemical tests. Corrosion occurs on Zn-coating anode and the reaction is



Since any aqueous solution in contact with air may contain dissolved oxygen, two cathodic reactions may occur, the evolution of hydrogen and the reduction of oxygen,



The corrosion rate of zinc depend on both the cathodic reactions but since the $\text{H}^+ - \text{H}_2$ exchange current density is very high on platinum, the corrosion rate mostly depends on hydrogen evolution reaction.

The cathodic polarization curves for both zinc and zinc-nickel alloy coatings at two different concentrations of NaCl are shown in Fig. 4.9. It is seen that the cathodic polarization behaviour of both coatings are similar. Increasing sodium chloride concentration is seen to increase the rate of cathodic reaction. This is consistent with the fact that increasing sodium chloride concentration increase the rate of anodic reactions too as described earlier.

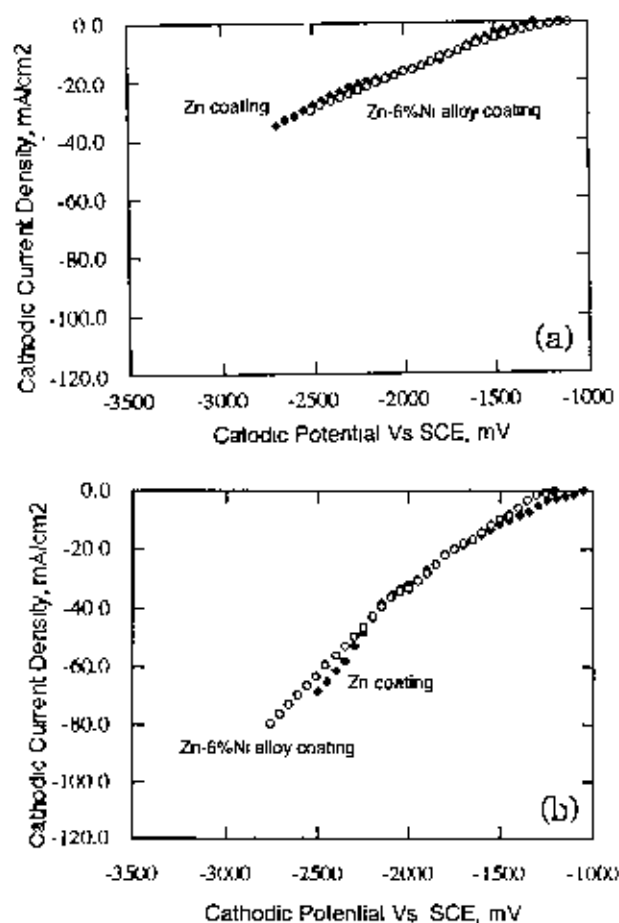


Fig. 4.9 Cathodic polarization curves for zinc and zinc-6% nickel alloy coatings in (a) 1.5% and (b) 4.5% NaCl solution.

Fig.4.10 shows the anodic polarization curves of pure zinc and Zn-6%Ni alloy coatings in 3wt% NaCl solution containing different percentage of Na_2S . The polarization curves moves upward as the Na_2S concentration increases from 0.1% to 0.2%. It is seen that the addition of 0.1% Na_2S decreases the anodic current density at zero applied potential. Comparison of Fig-4.10(a) with 4.8(b) also shows that in the range of potential studied. sodium chloride solution containing 0.1% Na_2S is less corrosive than the solution without Na_2S . However, further increase in Na_2S concentration to 0.2% increases the corrosiveness of the solution. Anodic current densities at zero applied potential on both zinc and Zn-Ni alloy for various Na_2S addition are listed in Table 4.6.

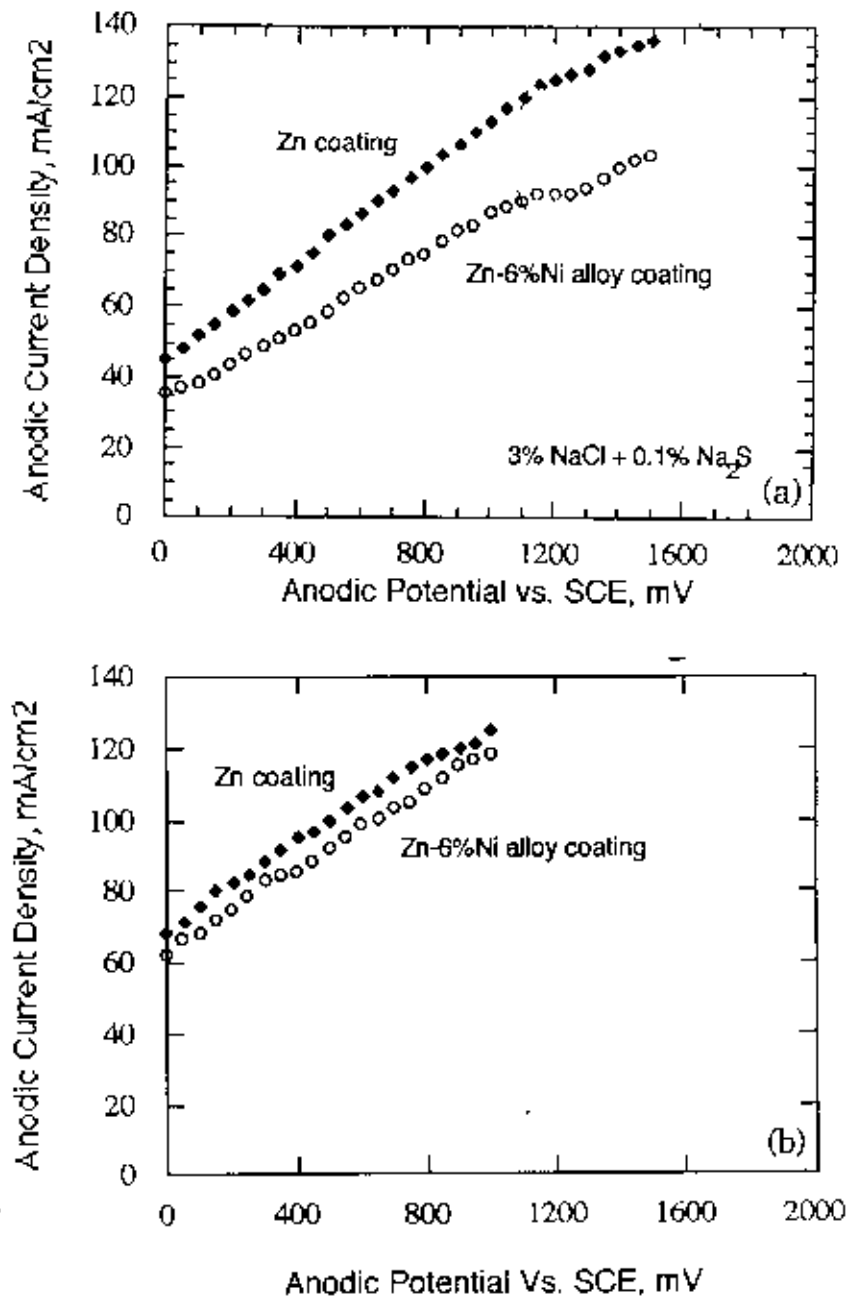


Fig. 4.10 Anodic polarization curves of pure zinc and zinc-6% nickel alloy coatings in 3 wt% NaCl solution containing (a) 0.1% Na₂S and (b) 0.2% Na₂S.

It is observed that at zero applied potential the anodic current density for 0.1% Na_2S addition is lower than that for 0.0% Na_2S . It may be mentioned that cathodic current densities were also lower in solution containing 0.1% Na_2S .

The lowering of corrosion rate at intermediate Na_2S concentration could be linked to the formation of a uniform corrosion product at this concentration. Maali et al³⁰ reported that the corrosion rate of mild steel decreases at an intermediate concentration of Na_2S and then increases as the Na_2S content of the NaCl based corrosion medium increases. They showed that the corrosion products that formed at intermediate concentration was uniform and protective. At higher Na_2S concentration, formation of loose, porous and nonprotective corrosion product led to accelerated corrosion of mild steel. Further work is necessary to identify the exact reason of a decrease in corrosion rate of zinc and zinc-nickel alloy coating at intermediate concentration of Na_2S in the salt solution.

Table 4.6 Anodic current densities at zero applied potential in solution containing NaCl and different amount of Na₂S.

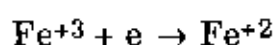
%NaCl	%Na ₂ S	Anodic current density at zero applied potential mA/cm ²	
		Zn	Zn-Ni
3.0	0.0	50.0	41.6
3.0	0.1	45.0	35.0
3.0	0.2	68.3	61.6

The effect of FeCl₃ concentration in corrosion medium (3% NaCl) on the anodic polarization behavior of zinc and Zn-Ni alloy coating is shown in Fig. 4.11. At high concentration FeCl₃ (viz.1%), the anodic polarization curves becomes steeper. Comparing Fig. 4.8(b) is with Fig. 4.11, it is observed that the presence of ferric chloride in the medium increases the corrosion rate of both coatings. The increased corrosion rate is particularly noticeable at 1% FeCl₃. The anodic current density at zero applied potential is particularly high at 1% FeCl₃ as can be seen in Table 4.7. At all concentrations of FeCl₃, zinc-6% nickel alloy coating is found to be more corrosion resistant than zinc coating.

Table 4.7 Anodic current densities at zero applied potential in solution containing NaCl and different amount of FeCl₃.

%NaCl	%FeCl ₃	Anodic current density at zero applied potential mA/cm ²	
		Zn	Zn-6%Ni
3.0	0.0	50.0	41.6
3.0	0.1	51.6	45.0
3.0	0.5	51.6	46.6
3.0	1.0	58.3	45.0

The presence of ferric ion in the corrosion medium increase the corrosion rate because the overall cathodic reactions increase due to ferric ion reduction.



Since anodic and cathodic reactions occurring during corrosion are mutually dependent the coating corrodes more rapidly in the presence of FeCl₃. (Fig. 4.11).

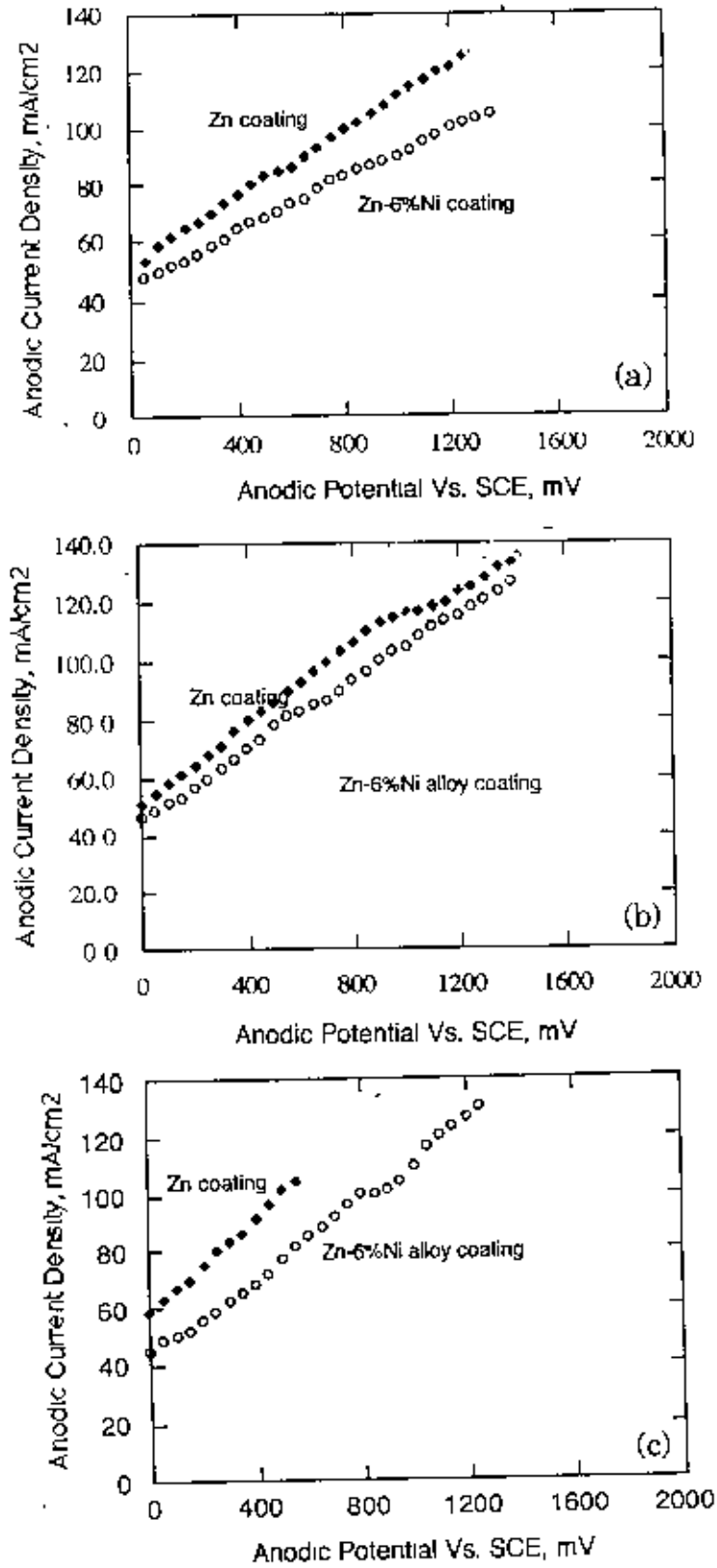


Fig. 4.11 Anodic polarization behavior of pure zinc and zinc-6% nickel alloy coatings in 3 wt% NaCl solution with FeCl₃ additions of (a) 0.1%, (b) 0.5% and (c) 1.0%.

The addition of ferric ion causes such pronounced change because of the relatively noble redox potential of $\text{Fe}^{+3} + e \rightarrow \text{Fe}^{+2}$ and its relatively high exchange current density of surface of metal(Pt).

Fig. 4.12 shows the anodic polarization behavior of zinc-nickel alloy coating in the as-deposited and annealed condition in 3% NaCl solution.

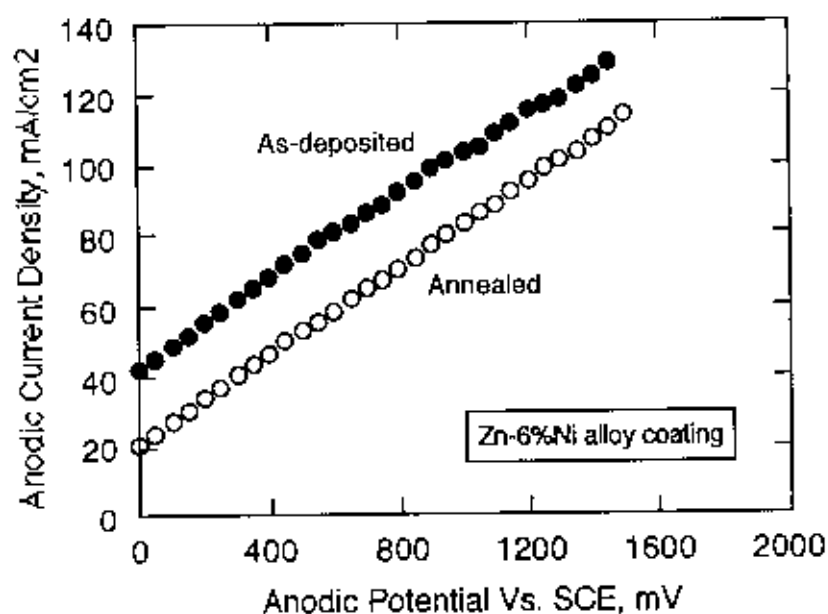


Fig. 4.12 Anodic polarization curves for zinc 6% nickel alloy coatings in the (a) as-deposited and (b) annealed condition in 3% NaCl solution.

It is observed that the anodic current densities for the annealed coatings at the zero applied potential are smaller than the corresponding values for the as-deposited coatings (Table 4.8).

Table 4.8 Anodic current densities of pure zinc and zinc-nickel alloy at zero applied potential.

Coating type	Anodic current density at zero applied potential, mA/cm ²	
	As-deposited	Annealed
Zn	50	26
Zn-6%Ni	41.6	20

The anodic polarization curve for annealed coating is found to lie below that for as-deposited coating. This means that annealed coating of zinc-nickel alloy are more corrosion resistant than as-deposited coatings.

It has been found aheads (@ 4.1.4) that there is a clear difference in X-ray diffraction patterns of coatings in the as-deposited and annealed conditions. As-deposited coatings are in a stressed/microcrystalline state and the resulting XRD pattern contains fewer and broader peaks. Annealing is believed to relieve the internal stress of the coatings as evidenced by the increase in the number of peaks and their sharpening. It is thus concluded that stress relieving by annealing increases the corrosion resistance of zinc-6% nickel alloy coating.

Anodic polarization behaviour of zinc and zinc-nickel alloy coatings were investigated by Giridhar and Ooij²⁹. They observed a passive region in the anodic polarization curves for both zinc and zinc-nickel alloy coatings. However no such passive region was observed in the present study. It may be mentioned that the coating thickness used by Giridhar and Ooij was in the range of 0.4-2.0 μm . At this small thickness, steel substrate was exposed during the polarization run. At the exposed areas, precipitation of zinc corrosion products (oxide, hydroxide and/or hydroxy chlorides of zinc) could occur³¹. This is because these exposed steel areas would act as cathodic sites where OH^- ions would generate from the reduction of oxygen resulting in an increase in pH. This screening of the exposed areas by zinc corrosion product led to a passive region in the polarization curve of Giridhar and Ooij. In the present study, rather thick (30 μm) layers of zinc and zinc-nickel alloy coatings were used. During anodic polarization measurement these thick coatings acted as bulk zinc and therefore did not show any passive region.

CHAPTER: FIVE

SUMMARY AND CONCLUSION

Zinc coatings have traditionally been used to protect steel structures and components from atmospheric and aqueous corrosion. Zinc-nickel alloy coatings have drawn considerable interest in recent years because of their improved corrosion resistance as compared with zinc coatings. In the present work, attempt has been made to investigate the electrodeposition of zinc-nickel alloy coatings and to study their corrosion behaviour. Deposition of pure zinc coating was also done and its corrosion behaviour studied for comparison purposes.

The deposition of Zn-Ni alloy coating on mild steel was carried out galvanostatically at current densities of 40, 60 and 80 mA/cm². Sulphate based plating baths of various formulations with pH range of 2-4 were utilized for the deposition at two different temperatures viz. 25 and 45°C. Electroplated coating of pure zinc from a bath containing Zn-sulphate was also made under the same condition.

The Zn-Ni coating was chemically analysed for nickel content mainly by atomic absorption spectroscopy (AAS). Conventional wet chemical analysis was also performed in some cases for comparison purposes. The thickness of the coating was determined under an optical microscope after polishing the cross-sectional substrate. X-ray diffraction studies were carried out on zinc-nickel alloy coatings in the as-deposited and annealed conditions.

In the present study the composition of the deposit was found to be affected by different parameters. The effect of increasing temperature at a given current density was to increase the nickel content of the deposits. It was observed that the nickel content of the deposits was independent of current density for baths containing 32% and 47% nickel ion. But for bath with 63% nickel ion, an increase in nickel percentage in the deposits was observed at higher current densities.

Anomalous type of codeposition was observed in the zinc-nickel system, i.e. nickel (more noble metal) percentage in the deposit was always lower than the nickel percentage in the bath. It was also seen that nickel percentage in the deposit increased linearly with increasing nickel percentage in bath. The pH of the plating bath was found to have a large effect on the quality of the zinc-nickel alloy deposits. In the pH range of 2-4, uniform and adherent coatings were obtained. At pH > 4, coatings became nonadherent and brittle; while at pH < 2, deposit was seen to form near the edge of the substrate and middle portion of the substrate remains bare.

The XRD patterns of as-deposited zinc and Zn-6% Ni alloy coating exhibited peaks of η and γ phases respectively. Upon annealing, the XRD peaks became sharper and additional peaks of γ -phase appeared in the case of Zn-6% Ni coating.

Tests for corrosion of both pure zinc and Zn-6% Ni alloy coatings on mild steel were made using immersion and electrochemical test. In immersion test, the coated substrates of area 3cm x 2cm exposed

were dipped in salt water (3% NaCl) solution as well as in hot-water. The progress of the corrosion was followed by visual examination and the time taken to form both white and red rust. Weight loss of the coated substrate was also recorded. Electrochemical corrosion test were made by using a Potentiostat in a conventional three electrode cell. During the tests, applied potential was incremented by 50 mV and the corresponding current density measured. Both anodic and cathodic polarization behaviour were recorded. The tests were performed in NaCl solution of various compositions with or without the addition of Na_2S and FeCl_3 .

For corrosion test, the Zn-Ni alloy coating obtained from bath containing 32% nickel ion (Bath-I) at current density 60 mA/cm^2 were chosen. The nickel content of the deposit was 6%. Thickness of both pure zinc and alloy coating was $30 \mu\text{m}$.

During the hot-water immersion test, no red rust was formed and it is concluded that the coatings used in the present study were uniform, pore free and continuous. Because spots of red rust were expected to form if the coatings were porous.

In salt water immersion test it was found that time taken to form both white and red rust on Zn-Ni alloy coating was longer than that on pure zinc. It took 120 days to form red rust on Zn-6%Ni alloy coating whereas it took only 55 days for pure zinc. But on bare mild steel red rust formed only after two days.

From the rest potential measurement it was seen that both zinc and zinc-nickel alloy coatings were less noble than mild steel. Presence of Na_2S and FeCl_3 was seen to shift the rest potential of both samples.

Anodic polarization behaviour shows that anodic current density on pure zinc coating was always higher than that on Zn-6%Ni alloy. This means that the corrosion rate of pure zinc in every corrosion medium was greater than that of Zn-6%Ni alloy coating. As the concentration of NaCl solution increased the corrosion rate of both zinc and Zn-6%Ni alloy increased.

It was seen that addition of 0.1% Na_2S decreased the anodic current density. Thus NaCl solution containing 0.1% Na_2S was less corrosive than the solution without Na_2S . The reason of this decrease in corrosion rate could be the formation of a uniform corrosion product. However further increase in Na_2S concentration to 0.2% increased the corrosiveness. The presence of ferric ion in the corrosion medium increased the corrosion rate of both coatings. The increased corrosion rate was particularly noticeable at 1% FeCl_3 .

The corrosion resistance of Zn-6%Ni alloy coatings increased upon annealing. XRD pattern showed that as-deposited coatings contained fewer and broad peaks but annealed coating contained sharper peaks. This was because of relief of internal stress. It is thus concluded that stress relieving by annealing increases the corrosion resistance of Zn-6%Ni alloy coatings.

References

1. J.W. van Zee and E.J. Rudd, *J. Electrochem. Soc.*, 135 (1988), p. 485C.
2. D.E. Hall, *Plat. and Surf. Finish.*, 70-71 (1983), p. 59.
3. R. Albalat, E. Gomez, C.Muller, M. Sarret, E. Valles and J. Pregones, *J. Appl. Electrochem.* 20, (1990) p. 635.
4. J. Giridhar and W.J. van Ooij, *Surf. Coat. Technol.*, 52 (1992) p. 17.
5. M. Pushpavanam, V. Raman, S. Jayakrishnan and B. A. Shenoi, *Advances in Electrochemical Science and Technology*, Oxford and IBH Publishing Co. Pvt. Ltd., New Delhi (1988), p. 155.
6. A. Brenner, *Electrodeposition of alloys Vols. I & II*. Academic press, New York (1963).
7. V. De Nora, *Studies of the electrodeposition of alloys of nickel-zinc*. *Met. ital.* 32 (1990) p. 187.
8. D. H. Schantz, *Electroplated corrosion proof metal articles and method of making the same*. U.S. Patent 2, 419, 231 (1987).
9. S.K. Pannikar and T.L Rama Char, *J. Sci. Ind. Research (India)* 17A 2, (1985) p. 95.
10. M.F. Mathias, C.M. Villa and T.W. Chapman, *J. Appl. Electrochem.* 20, (1990) p. 1.
11. E.P. Schoch and A. Hirsch, *Trans. Am. Electrochem. Soc.*, 11 (1907), p. 135.
12. W. von Escher, A. Tenne, F. Herrschel and M. Schade, *Z. Electrochem.* 22 (1916), p. 85.
13. B. Lustman, *Trans. Electrochem. Soc.* 84 (1943), p. 363.
14. ASTM G3-74, *Standard Recommended Practice for Conventions Applicable to Electrochemical Measurements in Corrosion Testing*, 1985 Annual Book of ASTM Standards, Vol. 03.02, ASTM, Philadelphia, Pennsylvania, (1985), p. 101.

15. NACE Publication 3D170, "Electrical and Electrochemical Methods for Determining Corrosion Rates (1984 Revision of 3D170)," National Association of Corrosion Engineers, Houston, Texas. (1984).
16. S.W. Dean, Jr. R.A. Woodroof. J. Nichols. "Electrochemical Methods for Evaluating Corrosion Inhibitors in Strong Acid Systems". Laboratory Corrosion Tests and Standards, ASTM STP 866, G.S. Haynes, R. Babioan, Eds., ASTM, Philadelphia, Pennsylvania, (1985), p. 228.
17. One example is the "Corrosion Rate Meter", Petrolite Corporation, Petroco Division, Houston, Texas.
18. T.Y. Chen, A. Moccari, D.D. Macdonald, "Development of Controlled Hydrodynamic Techniques for Corrosion Testing", MTI Final Report, Ohio State University, Columbus, Ohio, (1984).
19. ASTM D2776-79, Standard Test Methods for Corrosivity of Water in the Absence of Heat Transfer (Electrical Methods), 1984 Annual Book of ASTM Standards, Vol. 03.02. ASTM, Philadelphia, Pennsylvania, (1984), p. 72.
20. N.D. Greene, Experimental Electrode Kinetics, Rensselaer Polytechnic Institute, Troy, New York (1965).
21. R. L. Saur, R.P. Basco, Plating, Vol. 53, (1966), p. 33.
22. ASTM B627-79, Standard Method of FACT (Ford Anodized Aluminum Corrosion Test), 1983 Annual Book of ASTM Standards, Vol. 02.05m ASTM, Philadelphia, Pennsylvania, (1983), p. 489.
23. Md. Moniruzzaman, Study of the Mechanical Properties of Electrodeposited Zn-Ni alloy-Coating, M.Sc. Eng. Thesis, BUET, Dhaka 1995.
24. A. Knodler, Metalloberflache, 11, (1967), p. 321.
25. H. Fukushima, T. Akiyama, J. H. Lee, M. Yamaguchi, K. Higashi. Trans. J. Inst. Metals, 24(3), (1983), p. 125.

26. S. Swathirajan, J. Electroanal. Chem., 221, (1987), p. 211.
27. R.H. Parker, An Introduction to chemical Metallurgy, Pergamon Press, Oxford, (1967), p. 348.
28. A. J. Arvia and D. Posadas, in Encyclopedia of Electrochemistry of Elements, A. T. Bard (Editor), Marcel Dekker Inc, New York (1995), p. 300.
29. J. Giridhar and W.J. van Ooij, Surf. Coat. Technol, 53 (1992), p. 35.
30. A. Maali, M.Y. Taher, A.A. Agil and Rahmat, Proc. Int. Conf. Recent Advances in Materials and Mineral Resources, 3-5 May 1994, Penang, Malaysia.
31. I. Suzuki, Corros. Sci., 25 (1985), p. 1029.

